

Supporting Information for
**Subphthalocyanine–Tetracyanobuta-1,3-diene–Aniline
Conjugates: Stereoisomerism and Photophysical Properties**

Kim A. Winterfeld,^{‡a} Giulia Lavarda,^{‡b} Julia Guilleme,^{‡b} Dirk M. Guldi,^{*a} Tomás Torres,^{*bcd} and Giovanni Bottari^{*bcd}

^a Department of Chemistry and Pharmacy, Interdisciplinary Center for Molecular Materials (ICMM), Friedrich-Alexander-Universität Erlangen-Nürnberg, Egerlandstr. 3, 91058 Erlangen, Germany.

^b Departamento de Química Orgánica, Universidad Autónoma de Madrid, 28049 Madrid, Spain.

^c IMDEA-Nanociencia, Campus de Cantoblanco, 28049 Madrid, Spain.

^d Institute for Advanced Research in Chemical Sciences (IAdChem), Universidad Autónoma de Madrid, 28049 Madrid, Spain.

*e-mail: giovanni.bottari@uam.es; dirk.guldi@fau.de; tomas.torres@uam.es

[‡] These authors contributed equally to this work.

Table of Content

| | Page |
|--|------|
| 1. Materials and methods | S-2 |
| 2. Synthesis and characterization of (TCBD-aniline)-based SubPcs 1 and 2 | S-4 |
| 3. Detailed analysis of the chiral elements of (TCBD-aniline)-functionalized SubPcs 1 and 2 | S-20 |
| 4. Electrochemical characterization of (TCBD-aniline)-based SubPcs 1 and 2, and (ethynyl-aniline)-based SubPc 3 | S-27 |
| 5. Photophysical characterization of (TCBD-aniline)-based SubPcs 1 and 2, and reference compounds 3 and 5 | S-30 |
| 6. Supporting Information References | S-36 |

Abbreviations:

CIP = Cahn-Ingold-Prelog; CT = charge transfer; DCM = dichloromethane; DCTB = *trans*-2-[3-(4-*tert*-butylphenyl)-2-methyl-2-propenylidene]malononitrile; EtOAc = ethyl acetate; HRLSI-MS = high resolution laser spray ionization–mass spectrometry; MALDI-TOF = matrix-assisted laser desorption/ionization-time of flight; NMR = nuclear magnetic resonance; ppm = part per million; SubPc = subphthalocyanine; TCBD = tetracyanobuta-1,3-diene; TCNE = tetracyanoethylene; THF = tetrahydrofuran; TLC = thin layer chromatography.

1. Materials and methods.

Chemicals were purchased from commercial suppliers and used without further purification unless otherwise stated. Monitoring of the reactions has been carried out by thin layer chromatography (TLC), employing aluminum sheets coated with silica gel type 60 F254 (0.2 mm thick, E. Merck). Purification and separation of the synthesized products was performed by column chromatography, using silica gel (230–400 mesh, 0.040–0.063 mm, Merck). High Resolution Mass Spectrometry (HR-MS) spectra were recorded employing ESI Positive Q-TOF using a Bruker Maxis II, and Matrix Assisted Laser Desorption/ Ionization-Time of Flight (MALDI-TOF) using a Bruker Ultraflex III spectrometer, with a Nd-YAG laser. The different matrixes employed are indicated for each spectrum. Mass spectrometry data are expressed in *m/z* units.

¹H-NMR spectra were recorded on a Bruker AC-300 (300 MHz) and the temperature actively controlled at 298 K. In the ¹H-NMR spectra, the chemical shifts (δ) are measured in ppm relative to the correspondent deuterated solvent.

Steady state absorption spectroscopy was carried out with a Lambda 2 UV/Vis/NIR double beam spectrometer from PERKIN ELMER (190 to 1100 nm) and a Cary 5000 UV/Vis/NIR double beam spectrophotometer from VARIAN (175 to 3300 nm). The data was recorded with the software UV WinLab using a slit width of 2 nm and a scan rate of 480 nm/min and 600 nm/min, respectively. All measurements were performed without deaerating in a 10 × 10 mm Quartz cuvette (QS) with the respective solvent as reference.

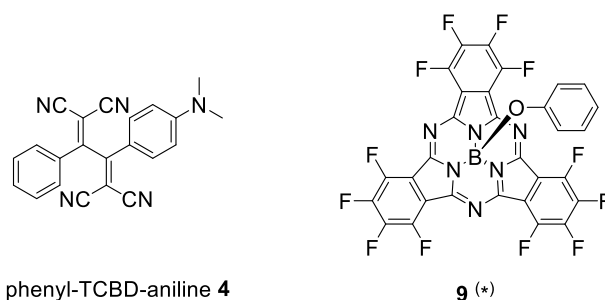
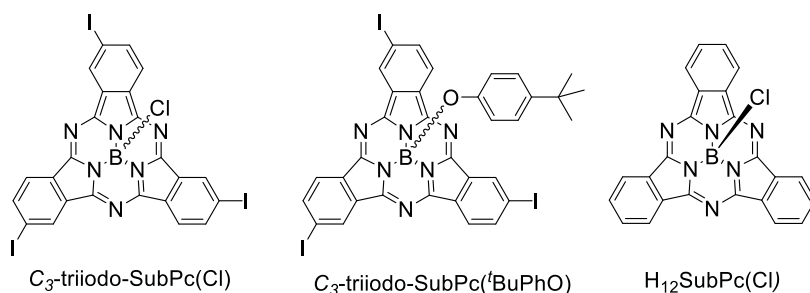
Steady state fluorescence measurements were performed with a FluoroMax[®]-3 fluorometer from HORIBA JOBIN YVON in a 10 × 10 mm Quartz cuvette (QS) without deaerating. All spectra were corrected for the instrument response. Data recording was

carried out with the software FluorEssence from HORIBA JOBIN YVON. A slit width of 2, 3, or 4 nm for both excitation and emission as well as an integration time of 0.1 or 0.2 s were applied. For determination of fluorescence quantum yields by the comparative method, a F₁₂SubPc axially substituted with a phenoxy ligand (**9**, see structure below) and showing a solvent-independent fluorescence quantum yield of 0.17¹ was used and the OD at the wavelength of excitation and beyond was kept below 0.1.

Transient absorption studies in the femto- to microsecond regime were carried out using a transient absorption pump/probe HELIOS/EOS system in combination with an amplified CPA-2110 Ti:sapphire laser (1 kHz, 150 fs pulse width, 775 nm output) from CLARK-MXR Inc. The excitation wavelength at 550 nm was generated with a non-collinear optical parameter (NOPA) from CLARK-MXR Inc. All measurements were conducted in a 2 mm Quartz cuvette (OS) under argon atmosphere. The data was recorded with the software HELIOS from Newport/Ultrafast Systems and fitted by multiwavelength (OriginLab, Northampton, MA) as well as global analysis. The latter was performed using the open-source software package GloTarAn, a Java based graphical user interface for the R package TIMP.^{2,3} TIMP is based on spectrotemporal parametrization assuming that the time dependent spectra are linear combinations of different absorption spectra of various species with their respective population profiles.⁴ An implemented response function accounting for dispersion and the coherent artifact were taken into account.

CV and SWV were performed in a single compartment glass cell with a three-electrode setup comprising a polished glassy carbon electrode as working electrode, a platinum wire as counter electrode, and a silver wire as pseudo reference electrode. The applied potential was controlled with a μ Autolab III/FRA2 potentiostat from METROHM and the current vs the applied potential was recorded by means of the software NOVA 1.10. All measurements were carried in an argon-saturated 0.2 M solution of *n*-Bu₄NPF₆ in DCM. The Fc⁺/Fc redox couple was used as internal standard.

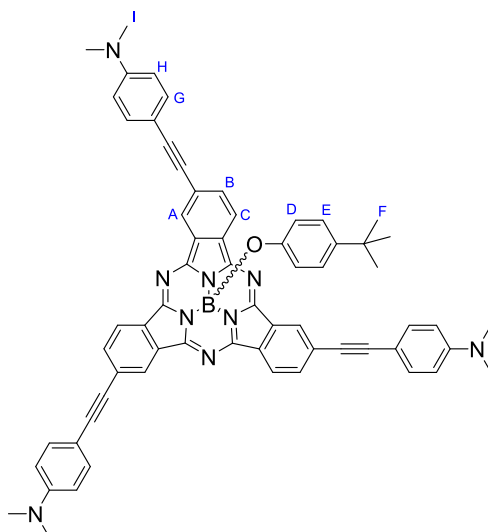
C₃-triiodo-SubPc(Cl)⁵ and C₃-triiodo-SubPc(^tBuPhO)⁶ (both obtained as a racemic mixture of the *M* and *P* isomers (*vide infra*)), H₁₂SubPc(Cl),⁷ and phenyl-TCBD-aniline **4**⁸ were prepared according to the synthetic procedure reported elsewhere and fully characterized.



(*) used as reference compound for fluorescence quantum yield measurements

2. Synthesis and characterization of (TCBD-aniline)-based SubPcs 1 and 2.

Synthesis and characterization of (ethynyl-aniline)₃-SubPc(^tBuPhO) 3



C_3 -triiodo-SubPc(^tBuPhO) (0.0325 mmol, 30 mg, 1 equiv), $PdCl_2(PPh_3)_2$ (0.0058 mmol, 4.0 mg, 18 mol%), and CuI (0.0058 mmol, 1.1 mg, 18 mol%) were placed in a 25 mL two-neck round bottom flask. Subsequently, a solution mixture of THF/ Et_3N (3 mL, v:v = 5:1) was added. The mixture was degassed by three “freeze-pump-thaw” cycles and 4-ethynyl-*N,N'*-dimethylaniline (0.137 mmol, 19.9 mg, 4.2 equiv) added. The resulting

solution was stirred at room temperature for 16 h. After this time, the reaction was filtered through celite and the solvent was evaporated under reduced pressure. The crude was purified by column chromatography on silica gel using chloroform as eluent. The desired product was triturated with methanol to afford pure **3** as a dark blue solid in 79% yield.

¹H-NMR (400 MHz, CDCl₃): δ (ppm) = 8.95 (dd, ⁴J_{H-H} = 1.2 Hz, ⁵J_{H-H} = 0.8 Hz, 3H; H_A), 8.74 (dd, ³J_{H-H} = 8.2 Hz, ⁵J_{H-H} = 0.8 Hz, 3H; H_C), 7.97 (dd, ³J_{H-H} = 8.2 Hz, ⁴J_{H-H} = 1.2 Hz, 3H; H_B), 7.51 (d, ³J_{H-H} = 8.9 Hz, 6H; H_G), 6.78 (d, ³J_{H-H} = 8.9 Hz, 6H; H_H), 6.71 (d, ³J_{H-H} = 9.0 Hz, 2H; H_D), 5.35 (d, ³J_{H-H} = 9.0 Hz, 2H; H_E), 3.03 (s, 18H; H_I), 1.09 (s, 9H; H_F); **¹³C-NMR** (101 MHz, CDCl₃): δ (ppm) = 151.55, 150.56, 150.18, 143.77, 133.17, 132.53, 131.27, 129.24, 126.25, 125.86, 125.13, 122.14, 117.92, 112.00, 109.65, 94.23, 88.11, 77.48, 40.34, 33.97, 31.47; **MALDI-TOF MS** (DCTB): *m/z* 824.4 [M-axial ligand]⁺, 973.4 [M]²⁺; **HRLSI-MS**: Calculated for C₆₄H₅₂BN₉O; 973.4388, found: 973.4397; **UV/vis** (CHCl₃): λ_{max} (nm) (log ε) = 603 (5.07), 549 (sh), 442 (4.47), 394 (4.52), 329 (5.02).

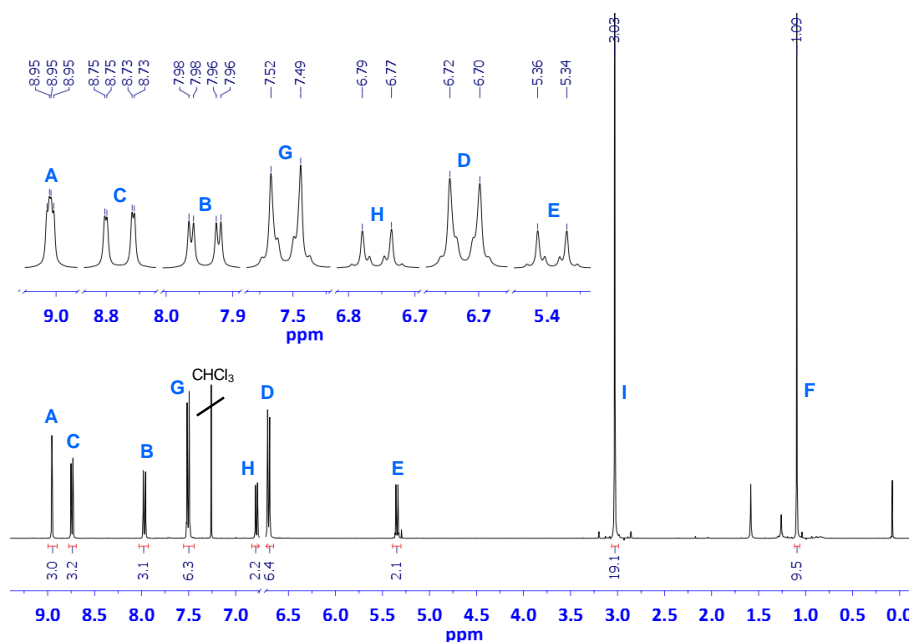


Figure S2.1. ¹H-NMR spectrum (CDCl₃) of (ethynyl-aniline)₃-SubPc(^tBuPhO) **3**. Inset: zoom of some of the proton peaks.

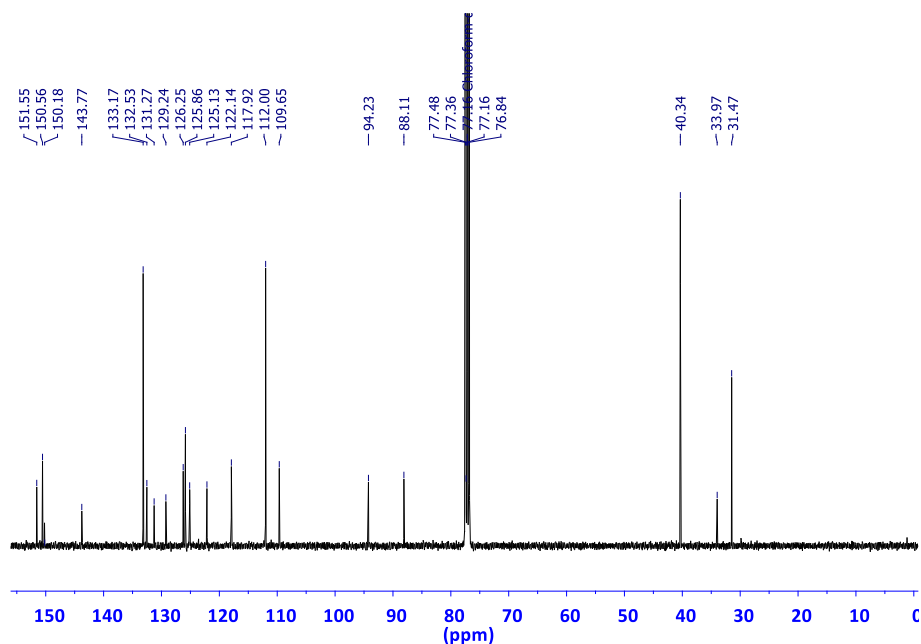


Figure S2.2. ^{13}C -NMR spectrum (CDCl_3) of (ethynyl-aniline) $_3$ -SubPc(BuPhO) **3**.

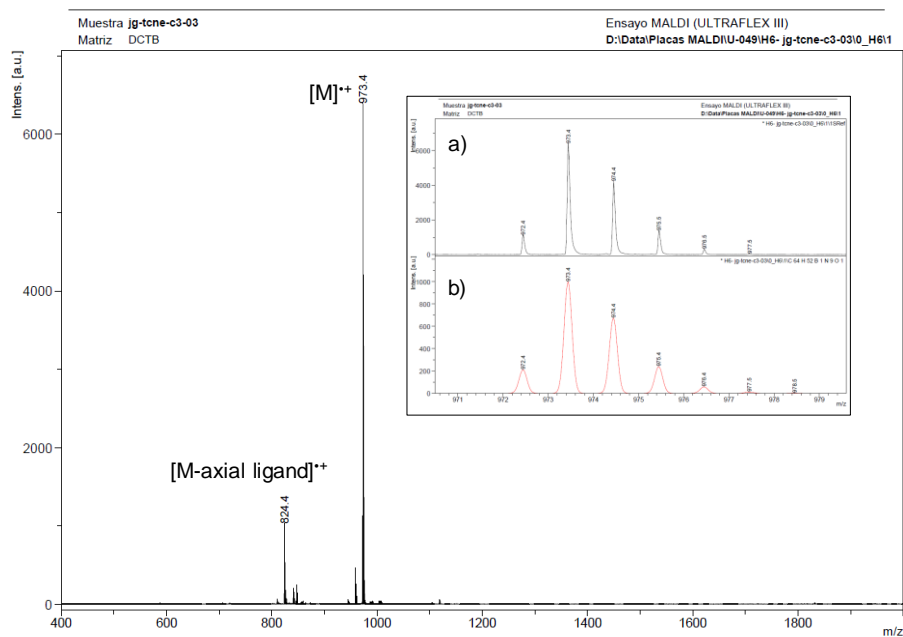


Figure S2.3. MALDI-TOF mass spectrum (in DCTB matrix) of (ethynyl-aniline) $_3$ -SubPc(BuPhO) **3**. Inset: a) isotopic resolution of the MALDI-TOF main peak at 973.4 m/z; b) calculated isotopic pattern for (ethynyl-aniline) $_3$ -SubPc(BuPhO) **3**.

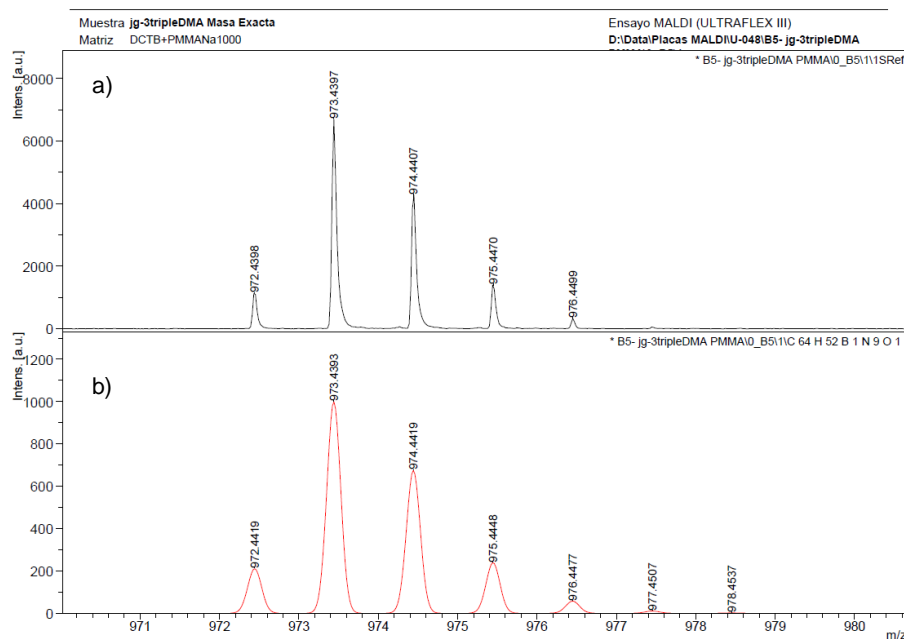
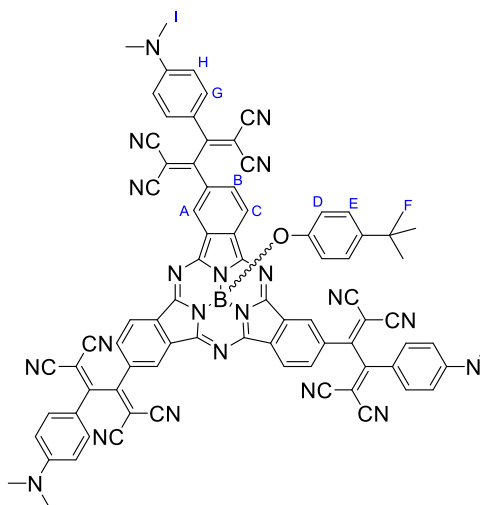


Figure S2.4. a) HRLSI-MS spectrum (in DCTB matrix) of (ethynyl-aniline)₃-SubPc(^tBuPhO) **3** in the region between 970 and 981 m/z; b) calculated isotopic pattern for (ethynyl-aniline)₃-SubPc(^tBuPhO) **3**.

Synthesis and characterization of (TCBD-aniline)₃-SubPc(^tBuPhO) **1**



(Ethynyl-aniline)₃-SubPc(^tBuPhO) **3** (0.03 mmol, 30 mg, 1 equiv) and TCNE (0.265 mmol, 34 mg, 7 equiv) were placed in a 25 mL two-neck round bottom flask equipped with a magnetic stirrer and a rubber seal. Then anhydrous THF (4 mL) was added and the solution stirred for 1 h at room temperature. After this time, the solvent was removed under reduced pressure and the resulting crude purified by column chromatography on silica gel employing CHCl₃/MeOH/pyridine (v:v:v = 98.9/1/0.1) as eluent. The solid

obtained was recrystallized using a DCM/hexane mixture. (TCBD-aniline)₃-SubPc(^tBuPhO) **1** was isolated as a dark green solid in 77% yield.

¹H-NMR (400 MHz, CDCl₃): δ (ppm) = 9.06 (d, ⁴J_{H-H} = 1.1 Hz, 3H; H_A), 9.00 (dd, ³J_{H-H} = 8.5 Hz, ⁵J_{H-H} = 0.4 Hz, 3H; H_C), 8.28 (dd, ³J_{H-H} = 8.5 Hz, ⁴J_{H-H} = 1.1 Hz, 3H; H_B), 7.89 (d, ³J_{H-H} = 9.4 Hz, 6H; H_G), 6.88 – 6.69 (m, 8H; H_H + H_E), 5.29 (d, ³J_{H-H} = 8.7 Hz, 2H; H_D), 3.19 (s, 18H; H_I), 1.08 (s, 9H; H_F); **¹³C-NMR** (101 MHz, CDCl₃): δ (ppm) = 167.23, 161.40, 153.50, 150.81, 150.23, 147.94, 143.39, 132.54, 132.26, 131.54, 129.85, 129.37, 124.91, 123.11, 123.08, 116.95, 116.34, 113.13, 112.35, 111.42, 110.83, 109.89, 87.98, 73.23, 39.12, 32.78, 30.11.; **MALDI-TOF** (DCTB): *m/z* 1208.4 [M-axial ligand]⁺, 1357.4 [M]⁺; **HRLSI-MS**: Calculated for C₈₂H₅₂BN₂₁O: 1357.4757, found:1357.4791; **UV/vis** (CHCl₃): λ_{max} (nm) (log ε) = 621 (4.83), 562 (shoulder), 465 (4.92), 341 (4.67), 314 (4.70).

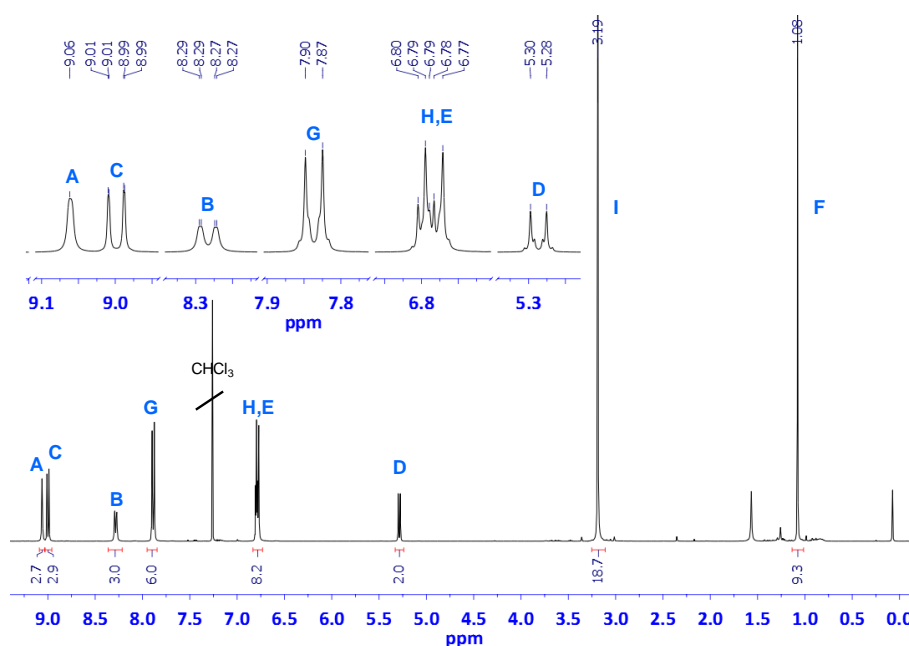


Figure S2.5. ¹H-NMR spectrum (CDCl₃) of (TCBD-aniline)₃-SubPc(^tBuPhO) **1**. Inset: zoom of some of the proton peaks.

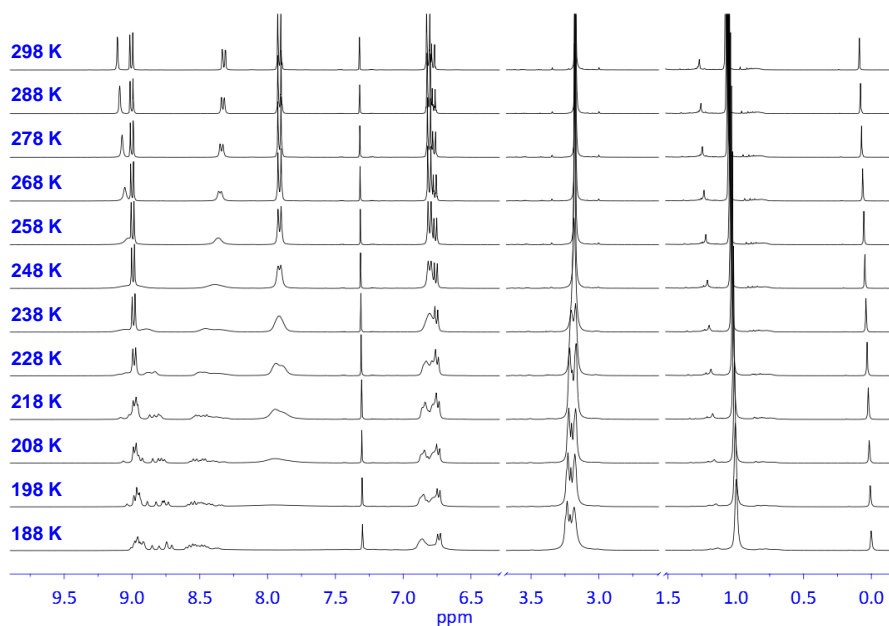


Figure S2.6. Variable-temperature $^1\text{H-NMR}$ spectra (CD_2Cl_2) of $(\text{TCBD-aniline})_3\text{-SubPc(BuPhO) 1}$.

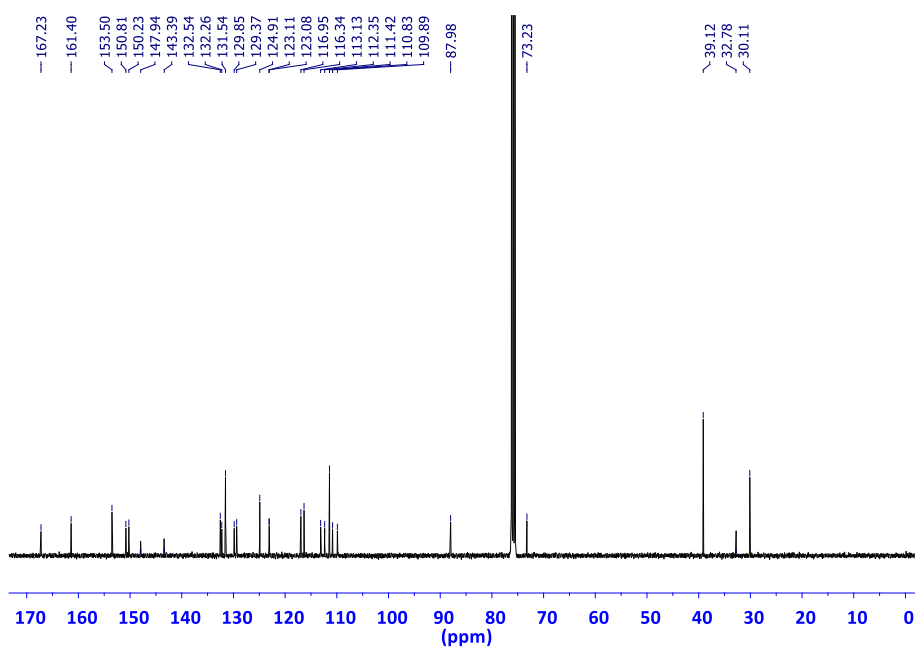


Figure S2.7. $^{13}\text{C-NMR}$ spectrum (CDCl_3) of $(\text{TCBD-aniline})_3\text{-SubPc(BuPhO) 1}$.

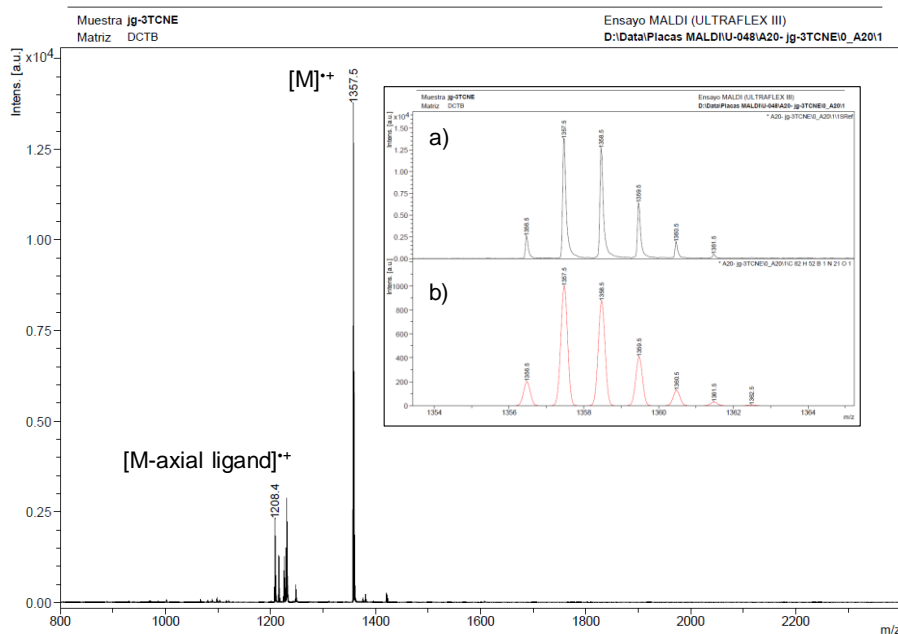


Figure S2.8. MALDI-TOF mass spectrum (in DCTB matrix) of (TCBD-aniline)₃-SubPc(BuPhO) **1**. Inset: a) isotopic resolution of the MALDI-TOF main peak at 1357.5 m/z; b) calculated isotopic pattern for (TCBD-aniline)₃-SubPc(BuPhO) **1**.

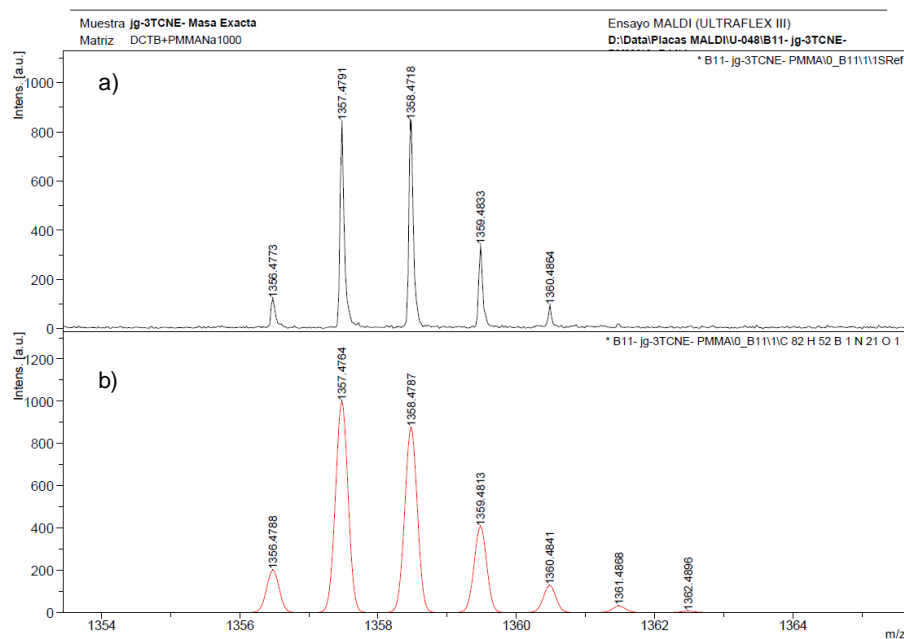
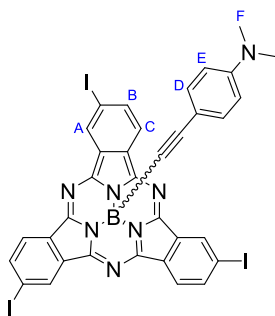


Figure S2.9. a) HRMS spectrum (in DCTB matrix) of (TCBD-aniline)₃-SubPc(BuPhO) **1** in the region between 1354 and 1365 m/z; b) calculated isotopic pattern for (TCBD-aniline)₃-SubPc(BuPhO) **1**.

Synthesis and characterization of triiodo-SubPc(ethynyl-aniline) **7**

Supporting Information for "Subphthalocyanine-Tetracyanobuta-1,3-diene-Aniline Conjugates: Stereoisomerism and Photophysical Properties" by Winterfeld et al.



EtMgBr (1M in THF, 0.055 mmol, 1.5 equiv) was added to a solution of 4-ethynyl-*N,N'*-dimethylaniline (0.074 mmol, 10.7 mg, 2 equiv) in anhydrous THF (1.5 mL) kept under argon. The solution was stirred at 60 °C for 1 h, and then transferred using a cannula to a degassed solution of *C*₃-triiodo-SubPc(Cl) (0.037 mmol, 30 mg, 1 equiv) in anhydrous THF (2 mL). The resulting solution was then stirred at 60 °C for 4 h observing, after this time, the complete disappearance of the SubPc starting material by TLC. Next, the solvent was evaporated and the crude dissolved in chloroform and washed with water. The organic phase was dried over anhydrous Mg₂SO₄, filtered and concentrated under reduced pressure. The resulting solid was purified by column chromatography on silica gel using toluene/EtOAc (v:v = 98:2) as eluent. The resulting solid was triturated with methanol to afford triiodo-SubPc(ethynyl-aniline) **7** as a dark blue solid in 59% yield.

¹H-NMR (400 MHz, CDCl₃): δ (ppm) = 9.20 (d, ⁴*J*_{H-H} = 0.9 Hz, 3H; H_A), 8.54 (dd, ³*J*_{H-H} = 8.3 Hz, ⁵*J*_{H-H} = 0.4 Hz, 3H; H_C), 8.19 (dd, ³*J*_{H-H} = 8.3 Hz, ⁴*J*_{H-H} = 0.9 Hz, 3H; H_B), 6.61 (d, ³*J*_{H-H} = 9.1 Hz, 2H; H_E), 6.25 (d, ³*J*_{H-H} = 9.1 Hz, 2H; H_D), 2.78 (s, 6H; H_F); **¹³C-NMR** (101 MHz, CDCl₃): δ (ppm) = due to the slow relaxation time of ¹³C nuclei in this compound, no ¹³C-NMR peaks were observed after a 16 h accumulation experiment; **MALDI-TOF** (DCTB): *m/z* 772.9 [M-axial ligand]⁺, 916.9 [M]⁺; **HRLSI-MS**: Calculated for C₃₄H₁₉BI₃N₇: 916.8929, found: 916.8936; **UV/vis** (CHCl₃): λ_{max} (nm) (log ε) = 575 (4.76), 556 (shoulder), 535 (4.23), 314 (4.60), 286 (shoulder).

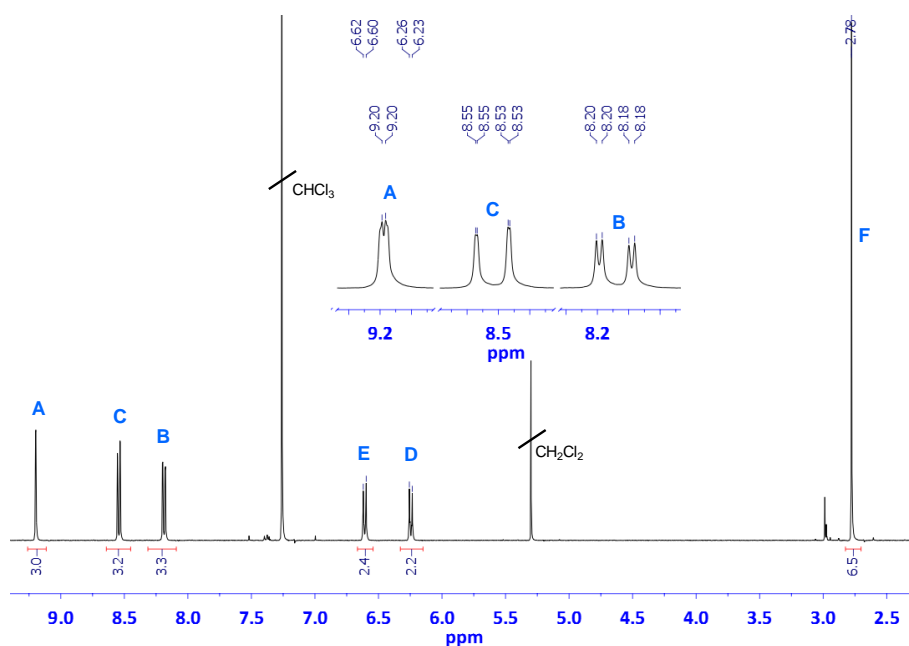


Figure S2.10. $^1\text{H-NMR}$ spectrum (CDCl_3) of triiodo-SubPc(ethynyl-aniline) **7**. Inset: zoom of some of the proton peaks.

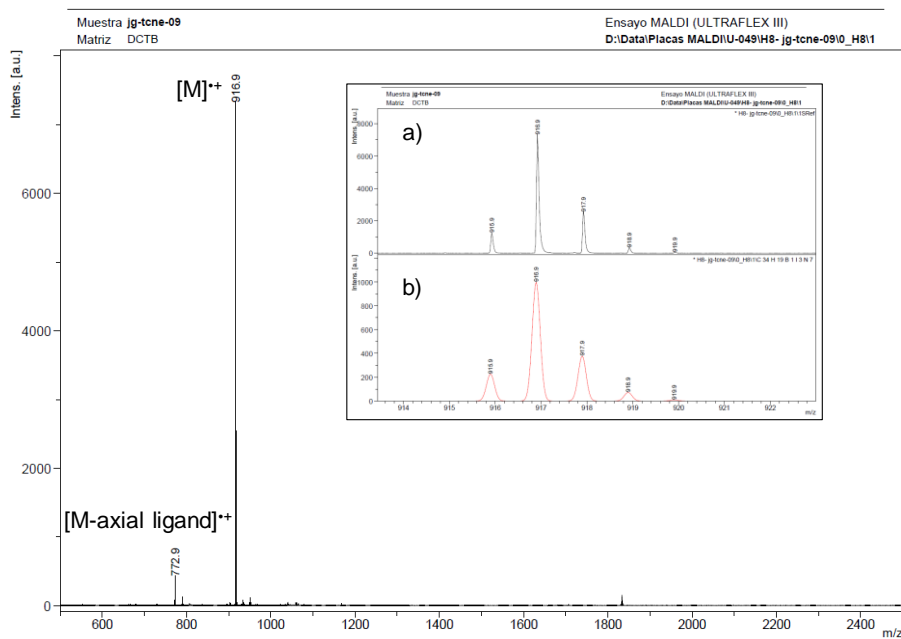


Figure S2.11. MALDI-TOF mass spectrum (in DCTB matrix) of triiodo-SubPc(ethynyl-aniline) **7**. Inset: a) isotopic resolution of the MALDI-TOF main peak at 916.9 m/z; b) calculated isotopic pattern for triiodo-SubPc(ethynyl-aniline) **7**.

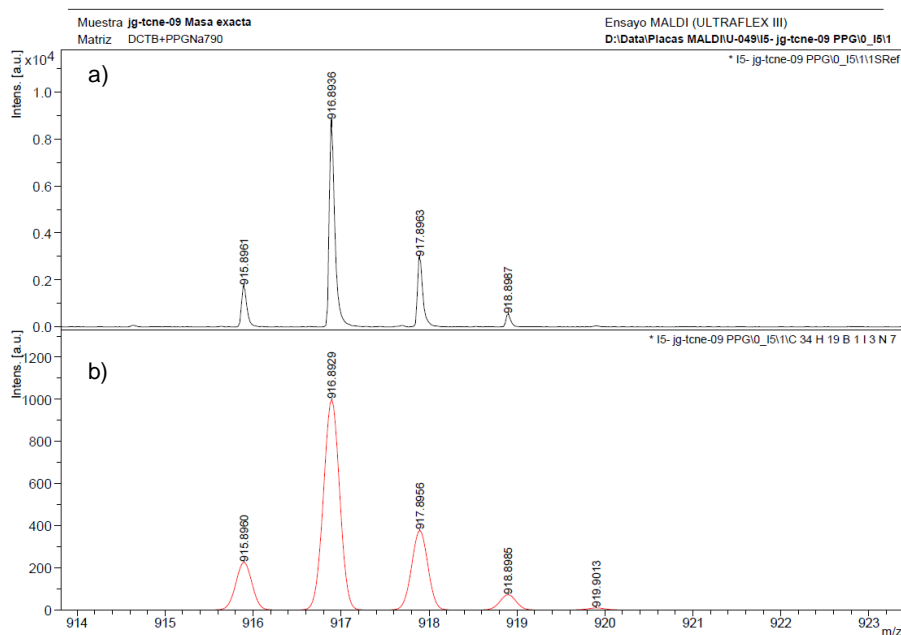
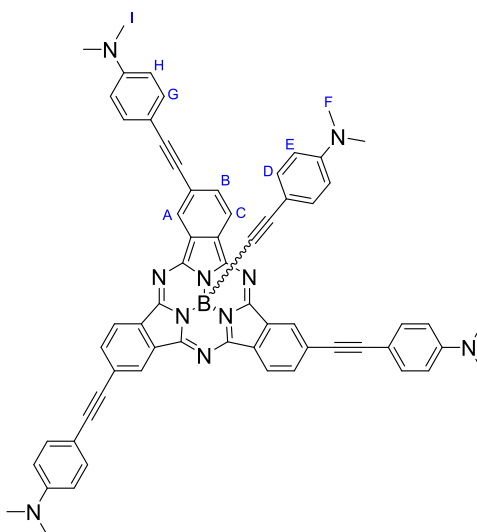


Figure S2.12. a) HRLSI-MS spectrum of triiodo-SubPc(ethynyl-aniline) **7** in the region between 914 and 923 m/z; b) calculated isotopic pattern for triiodo-SubPc(ethynyl-aniline) **7**.

Synthesis and characterization of (ethynyl-aniline)₃-SubPc(ethynyl-aniline) **8**



Triiodo-SubPc(ethynyl-aniline) **7** (0.014 mmol, 13 mg, 1 equiv), PdCl₂(PPh₃)₂ (0.0026 mmol, 1.8 mg, 18 mol%), and CuI (0.0026 mmol, 0.5 mg, 18 mol%) were placed in a 25 mL two-neck round bottom flask. Subsequently, THF/Et₃N (2 mL, v:v = 5:1) was added. The mixture was degassed by three “freeze-pump-thaw” cycles, and then 4-ethynyl-*N,N'*-dimethylaniline (0.05 mmol, 7.4 mg, 4.2 equiv) added to the solution which was stirred at room temperature for 16 h. After this time, the reaction was filtered through celite and the solvent evaporated under reduced pressure. The resulting was purified by column

chromatography on silica gel using chloroform as eluent. The isolated product was triturated with methanol to afford (ethynyl-aniline)₃-SubPc(ethynyl-aniline) **8** as a blue solid in 87% yield.

¹H-NMR (400 MHz, CDCl₃): δ (ppm) = 8.96 (dd, ⁴J_{H-H} = 1.2 Hz, ⁵J_{H-H} = 0.8 Hz, 3H; H_A), 8.75 (dd, ³J_{H-H} = 7.6 Hz, ⁵J_{H-H} = 0.8 Hz, 3H; H_C), 7.96 (d, ³J_{H-H} = 7.6 Hz, ⁴J_{H-H} = 1.2 Hz, 3H; H_B), 7.51 (d, ³J_{H-H} = 8.9 Hz, 6H; H_G), 6.71 (d, ³J_{H-H} = 8.9 Hz, 6H; H_H), 6.66 (d, ³J_{H-H} = 9.1 Hz, 2H; H_E), 6.26 (d, ³J_{H-H} = 9.1 Hz, 2H; H_D), 3.03 (s, 18H H_I), 2.78 (s, 6H; H_F); **¹³C-NMR** (101 MHz, CDCl₃): δ (ppm) = 150.54, 150.51, 150.50, 149.81, 133.15, 132.70, 132.31, 131.17, 130.38 129.21, 125.93, 125.02, 122.01, 112.00, 111.39, 109.74, 109.37, 93.97, 88.23, 40.34, 40.15; **MALDI-TOF** (DCTB): *m/z* 953.5 [M-CH₃]⁺, 968.5 [M]⁺, 1937.0 [2M]⁺; **HRLSI-MS**: Calculated for C₆₄H₄₉B₁N₁₀: 967.4266, found: 967.4233; **UV/vis** (CHCl₃): λ_{max} (nm) (log ε) = 605 (5.38), 555 (shoulder), 429 (4.84), 396 (4.95), 320 (5.44).

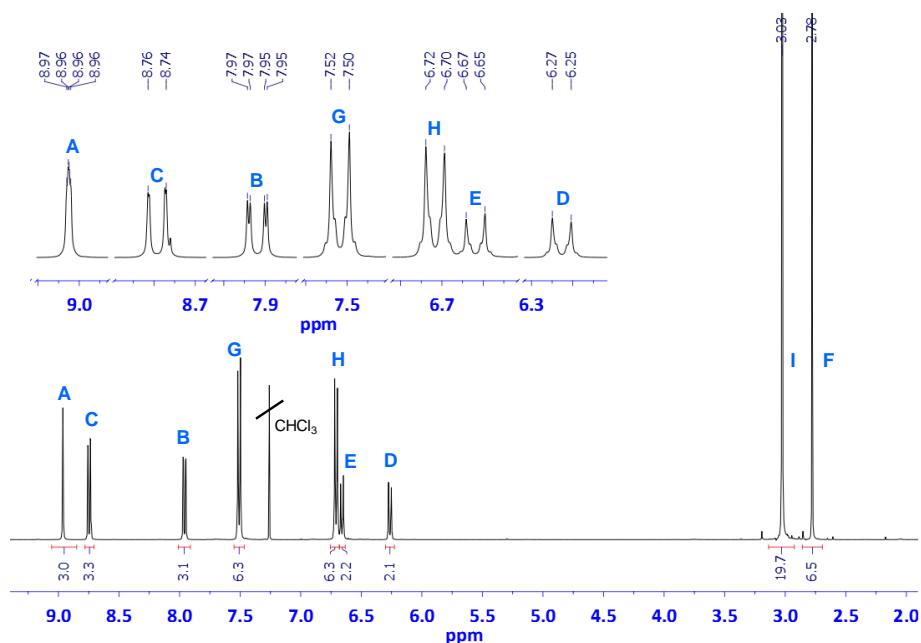


Figure S2.13. ¹H-NMR spectrum (CDCl₃) of (ethynyl-aniline)₃-SubPc(ethynyl-aniline) **8**. Inset: zoom of some of the proton peaks.

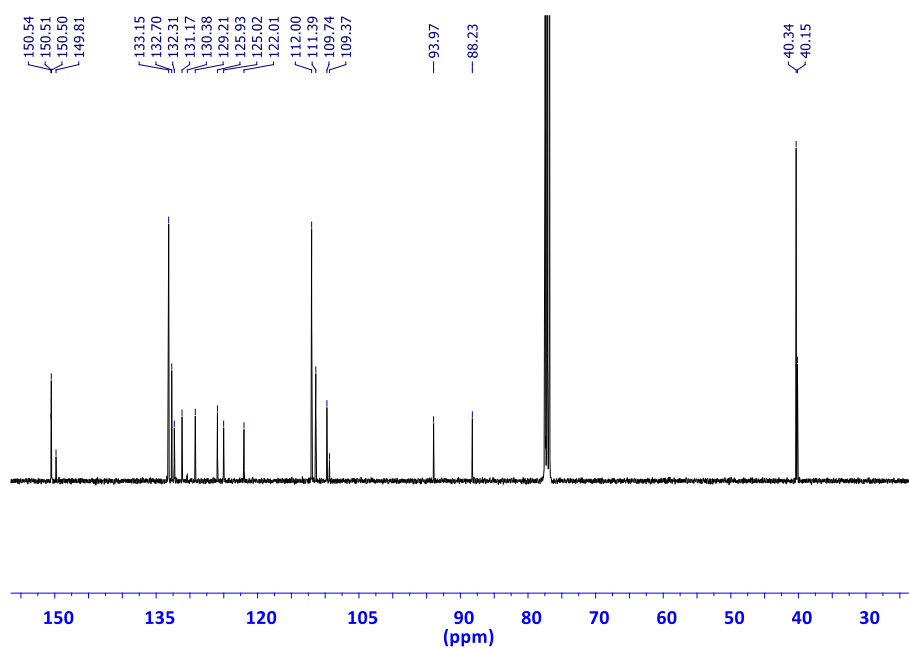


Figure S2.14. ^{13}C -NMR spectrum (CDCl_3) of (ethynyl-aniline) $_3$ -SubPc(ethynyl-aniline) **8**.

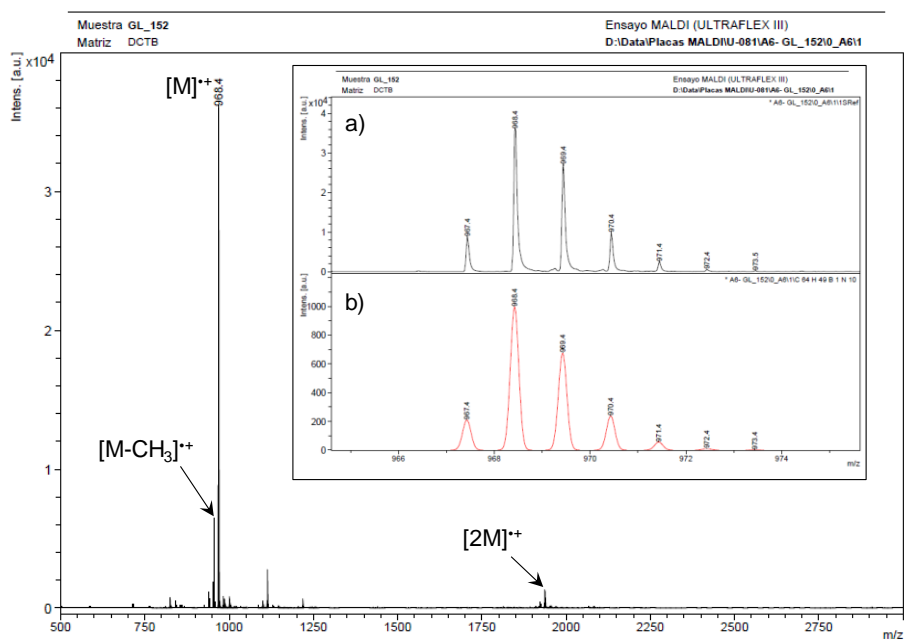


Figure S2.15. MALDI-TOF mass spectrum (in DCTB matrix) of (ethynyl-aniline) $_3$ -SubPc(ethynyl-aniline) **5**. Inset: a) isotopic resolution of the MALDI-TOF main peak at 968.4 m/z; b) calculated isotopic pattern for (ethynyl-aniline) $_3$ -SubPc(ethynyl-aniline) **8**.

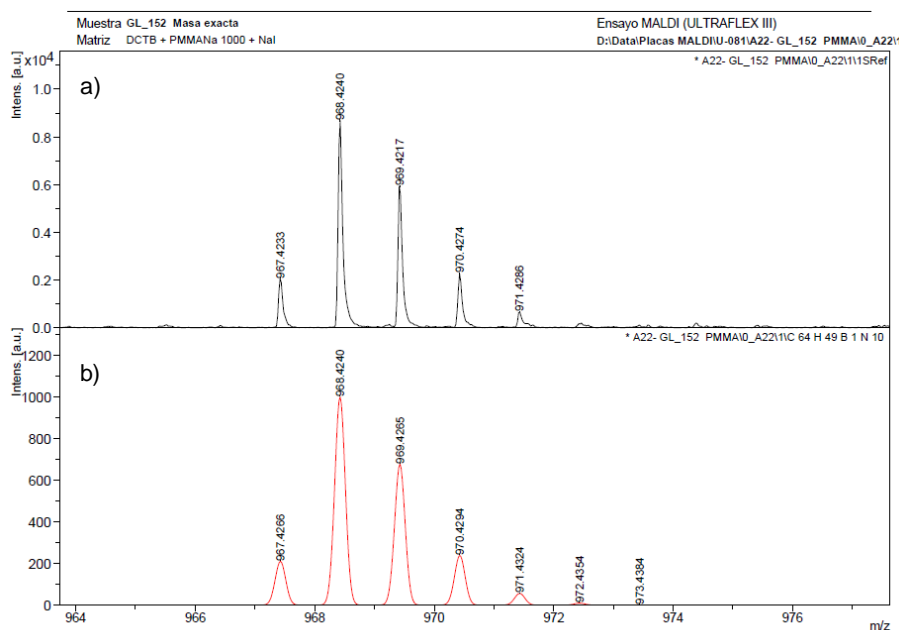
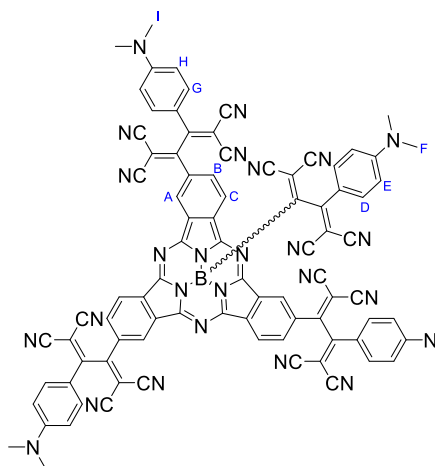


Figure S2.16. a) HR-MS spectrum of (ethynyl-aniline)₃-SubPc(ethynyl-aniline) **8** in the region between 964 and 977 m/z; b) calculated isotopic pattern for (ethynyl-aniline)₃-SubPc(ethynyl-aniline) **8**.

Synthesis and characterization of (TCDB-aniline)₃-SubPc(TCDB-aniline) **2**



(Ethynyl-aniline)₃-SubPc(ethynyl-aniline) **8** (0.012 mmol, 12 mg 1 equiv) and TCNE (0.059 mmol, 7.6 mg, 4.8 equiv) were placed in a 25 mL two-neck round bottom flask equipped with a magnetic stirrer and a rubber seal. Then anhydrous THF (3 mL) was added and the solution stirred for 1 h at room temperature. After this time, the solvent was removed under reduced pressure and the resulting crude purified by column chromatography on silica gel using CHCl₃/MeOH/pyridine (v:v:v = 98.9/1/0.1) as eluent. The isolated product was triturated with hexane to afford (TCDB-aniline)₃-SubPc(TCDB-aniline) **2** as a dark green solid in 40% yield.

Supporting Information for "Subphthalocyanine–Tetracyanobuta-1,3-diene–Aniline Conjugates: Stereoisomerism and Photophysical Properties" by Winterfeld et al.

¹H-NMR (400 MHz, CD₂Cl₂): δ (ppm) = 9.10 (d, ⁴J_{H-H} = 0.8 Hz, 3H; H_A), 9.08 (d, ⁴J_{H-H} = 0.8 Hz, 3H; H_A), 8.98 (dd, ³J_{H-H} = 8.4 Hz, ⁵J_{H-H} = 0.8 Hz, 3H; H_C), 8.94 (dd, ³J_{H-H} = 8.4 Hz, ⁵J_{H-H} = 0.8 Hz, 3H; H_C), 8.33 (dd, ³J_{H-H} = 8.4 Hz, ⁴J_{H-H} = 1.6 Hz, 3H; H_B), 8.29 (dd, ³J_{H-H} = 8.4 Hz, ⁴J_{H-H} = 1.6 Hz, 3H; H_B), 7.92 – 7.86 (m, 12H; H_G), 6.83 – 6.77 (m, 12H; H_H), 6.68 – 6.65 (m, 4H; H_E), 6.43–6.40 (m, 4H; H_D), 3.17 (s, 18H; H_I), 3.15 (s, 18H; H_I), 3.04 (s, 6H; H_F), 3.04 (s, 6H; H_F); **¹³C-NMR** (101 MHz, CD₂Cl₂): δ (ppm) = 168.77, 162.73, 155.43, 152.48, 152.31, 152.15, 134.89, 134.85, 133.53, 133.29, 131.71, 131.55, 131.15, 125.08, 124.92, 124.62, 118.49, 118.43, 115.05, 114.33, 113.08, 112.72, 112.27, 111.74, 90.29, 74.48, 74.44, 40.72; **MALDI-TOF** (DCTB): *m/z* 1481.4 [M]⁺, 1504.4 [M+Na]⁺; **HRLSI-MS**: Calculated for C₈₈H₄₉BN₂₆Na: 1504.4654, found: 1504.4685; **UV/vis** (CHCl₃): λ_{max} (nm) (log ε) = 635 (4.83), 586 (sh), 470 (5.13), 343 (4.83), 314 (4.83).

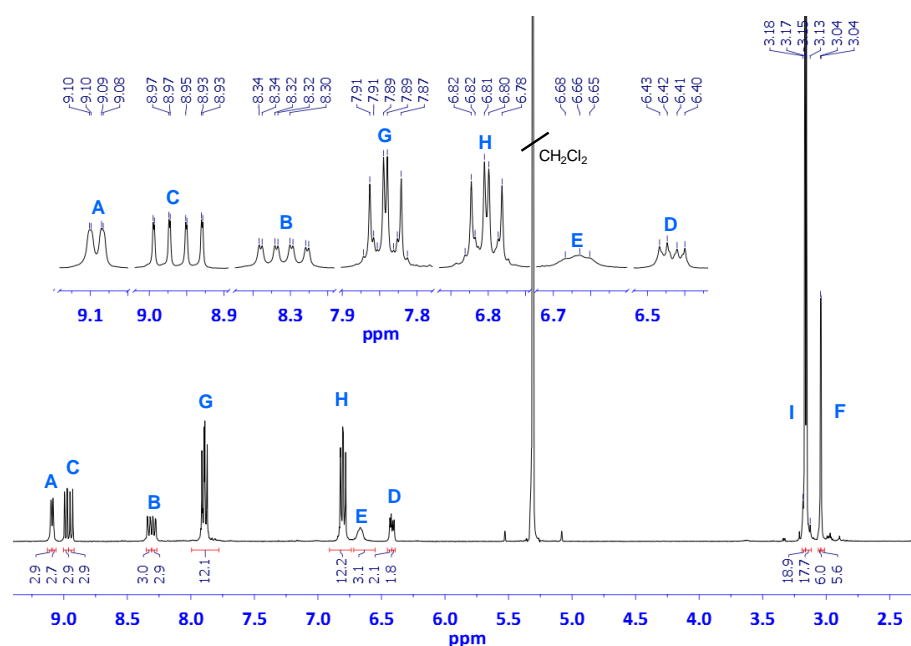


Figure S2.17. ¹H-NMR spectrum (CD₂Cl₂) of (TCDB-aniline)₃-SubPc(TCBD-aniline) **2**. Inset: zoom of some of the proton peaks.

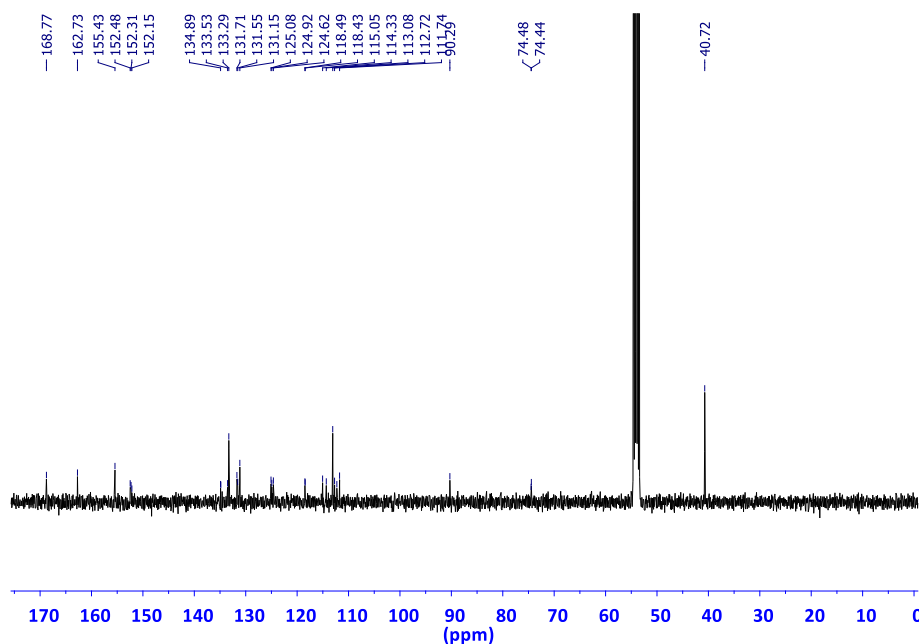


Figure S2.18. ^{13}C -NMR spectrum (CD_2Cl_2) of $(\text{TCDB-aniline})_3\text{-SubPc}(\text{TCDB-aniline})$ **2**.

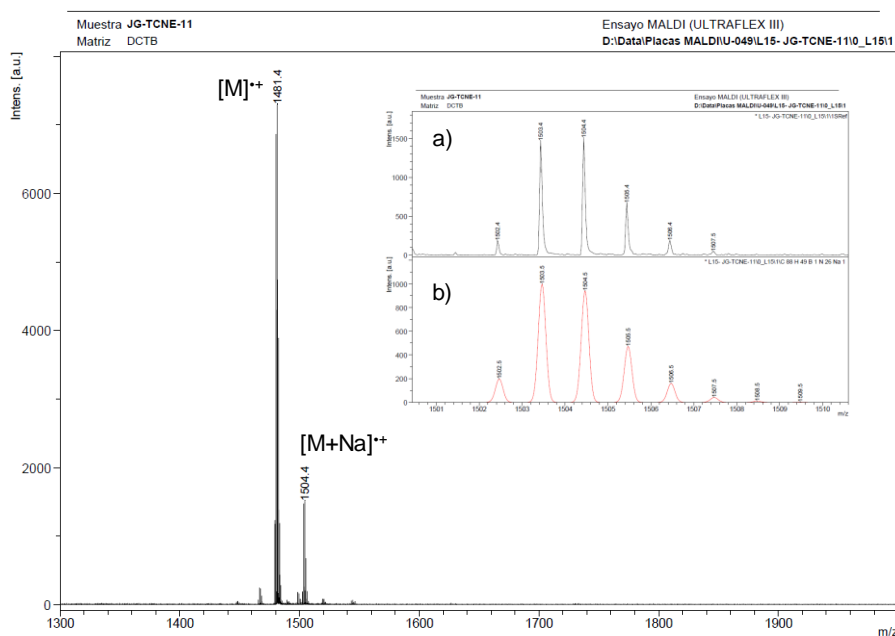


Figure S2.19. MALDI-TOF mass spectrum (in DCTB matrix) of $(\text{TCDB-aniline})_3\text{-SubPc}(\text{TCDB-aniline})$ **2**. Inset: a) isotopic resolution of the MALDI-TOF main peak at 1481.4 m/z ; b) calculated isotopic pattern for $(\text{TCDB-aniline})_3\text{-SubPc}(\text{TCDB-aniline})$ **2**.

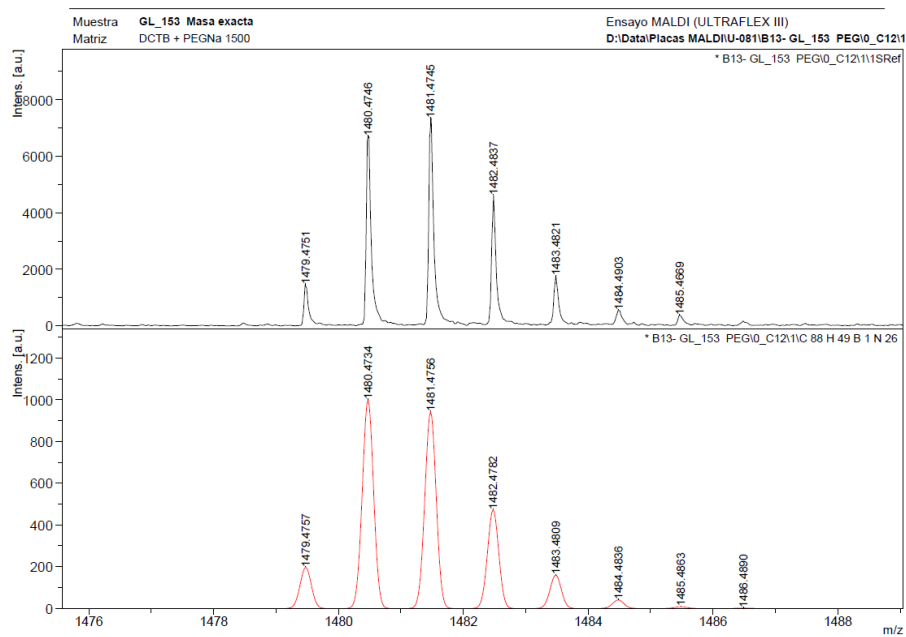


Figure S2.20. a) HR-MS spectrum of (TCDB-aniline)₃-SubPc(TCBD-aniline) **2** in the region between 1476 and 1490 m/z; b) calculated isotopic pattern for (TCDB-aniline)₃-SubPc(TCBD-aniline) **2**.

3. Detailed analysis of the chiral elements of (TCBD-aniline)-functionalized SubPcs 1 and 2.

As a consequence of their cone-shape structure, SubPcs presenting an achiral axial ligand and three achiral peripheral substituents attached to the macrocycle through a C_3 symmetric substitution pattern (as in the case of triiodo-SubPc(Cl) **5**) are obtained as a racemic mixture of two enantiomers, namely, *M* and *P* (Figures S3.1b and S3.1c, respectively). In order to assign the *M* and *P* configuration to a C_3 symmetric SubPc, a convention is followed. Step 1: the C_3 symmetric SubPc is placed having the axial ligand pointing towards the observer. Step 2: the rim atoms that rank highest in priority - according to the CIP rules - are identified. Step 3: from a rim atom ranking highest in CIP priority two opposite pathways are followed, one clockwise and the other counter-clockwise, until the first difference in CIP priority is encountered. Step 4: If the direction of travel from the rim atom ranking highest in CIP priority to the second higher CIP priority atom is clockwise, then the SubPc is designated as *P*; a SubPc requiring counter-clockwise travel is designated as *M* (Figure S3.1a). By this convention, the triiodo-SubPc(Cl) **5** pictured in Figure S3.1b,c would be designated as *M* (Figure S3.1b) or *P* (Figure S3.1c).

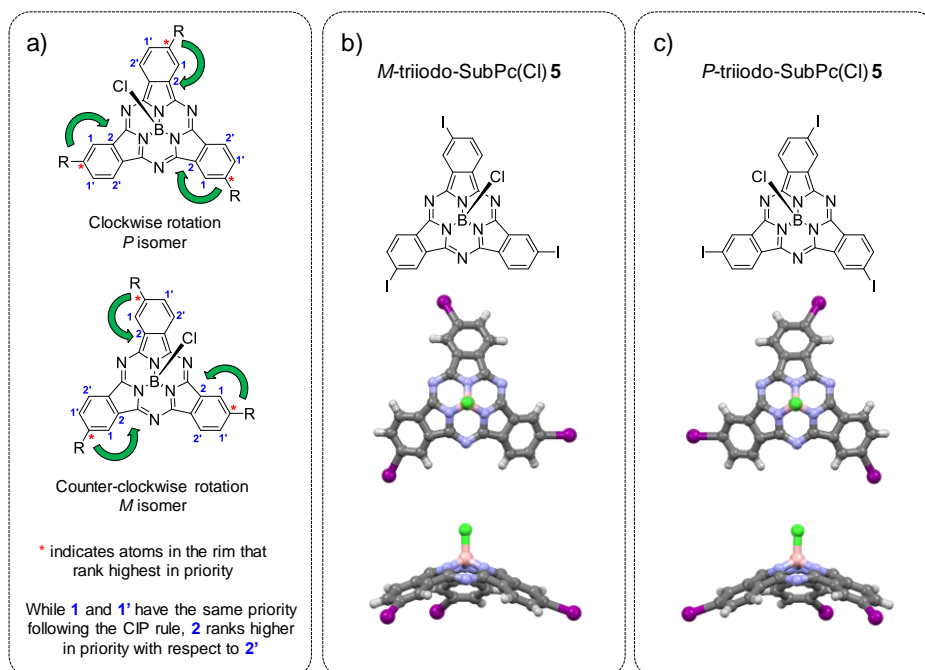


Figure S3.1. a) How to assign the *M* or *P* configuration of a generic C_3 -symmetric SubPc. Chemical (top) and molecular modelling structure ((middle) top- and (bottom) lateral view (with respect to the SubPc B-Cl bond)) of (b) *M* and (c) *P* enantiomers of triiodo-SubPc(Cl) **5**.

In the case of TCBD derivatives, two atropisomers, namely, R_a and S_a , should be considered. Each atropisomer possesses a chiral axis as a result of the hindered rotation around the $C_2(sp^2)-C_3(sp^2)$ bond of the butadiene moiety.

For compounds possessing axial chirality such as TCBD, the stereochemical labels R_a and S_a are assigned following these rules:

The TCBD unit is placed so as to have i) its chiral axis viewed end-on, and ii) the two "near" and two "far" substituents orthogonal between them (see Figure S3.2, as example). Next, among the two "near" substituents, the one with the highest priority is identified.* Then, the same process is repeated for the two "far" substituents and the group among them with the highest priority identified.* Finally, the R_a or S_a configurations are determined as a function of the clockwise (R_a) or anticlockwise rotation (S_a) when moving from the group with the highest priority among the two "near" substituents (1) to the other one (1') and then to the group with the highest priority among the two "far" substituents (2) (*i.e.*, $1 \rightarrow 1' \rightarrow 2$).†

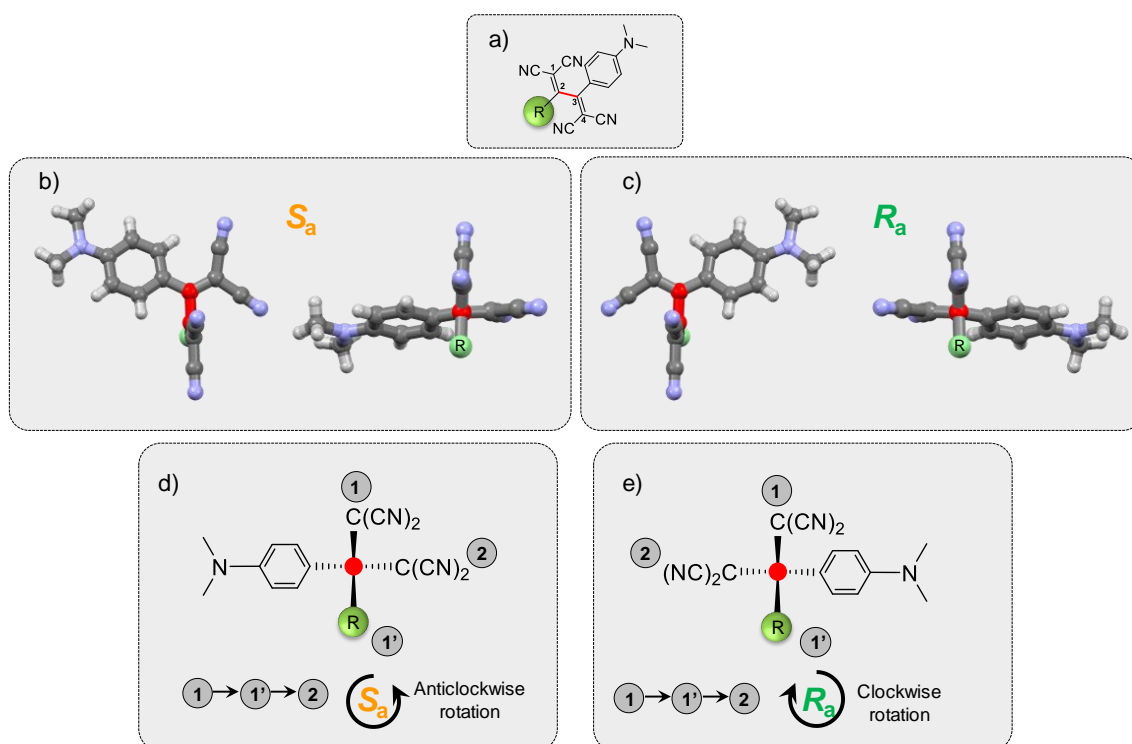


Figure S3.2. a) General molecular structure of a TCBD-aniline derivative, and numbering of the buta-1,3-diene fragment assuming that the R group has higher priority with respect to the aniline

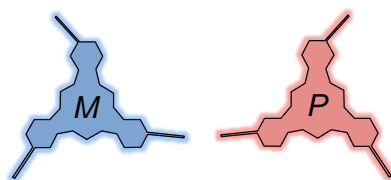
* The group priority is assigned following the CIP priority rules used for tetrahedral stereocenters.

† In the case of axial chirality, the stereodescriptor R_a or S_a is reached independently of the direction one sights down the chiral axis.

group.* b,c) Views of the molecular modeling structures of a generic TCBD-aniline derivative visualized perpendicular to (left) and along the (right) butadiene C₂-C₃ axis (colored in red). As a result of the hindered rotation around the C₂-C₃ bond of the TCBD fragment (colored in red in a-c) which is a chiral axis, two atropisomers, namely, S_a (b) and R_a (c), are formed. For both atropisomers, the R_a (d) or S_a (e) configuration is assigned based on the priority among i) the two substituents attached to the C₂ carbon atom (marked as a red dot) (in this case, the dicyanovinyl group and the R group),[‡] and ii) the two substituents attached to the C₃ carbon atom (eclipsed by the C₂ carbon) (in this case, the dicyanovinyl group and the N,N'-dimethyl-aniline moiety) of the TCBD unit.*

In order to figure out the possible stereoisomers that could be expected for a racemic mixture of the *M* and *P* isomers of (TCBD-aniline)₃-SubPc(^tBuPhO) **1** and (TCBD-aniline)₃-SubPc(TCBD-aniline) **2**, a simplified model is proposed.

1) Since **1** and **2** possess a C₃-symmetry peripheral functionalization pattern (not considering the possible stereochemical features of the peripheral groups) resulting from the use of C₃-symmetric triiodo-SubPc(Cl) **5** as common precursor for both syntheses, the *M* and *P* SubPc isomers are considered.



2) Each of the three peripheral TCBD units is represented as a red arrow pointing up or a blue arrow pointing down. A red arrow pointing up means that the N,N'-dimethyl-aniline moiety of the TCBD is pointing to the same side to which the SubPc axial ligand points to, whereas a blue arrow pointing down means that the N,N'-dimethyl-aniline moiety of the considered TCBD is pointing at the opposite side to which the SubPc axial ligand points to.



3) The arrows, pointing either up or down, are filled with either orange or green color. An arrow filled with orange color means that the configuration of the TCBD unit is S_a, whereas an arrow filled with green color means that the configuration of the TCBD unit is R_a. It is important to mention here that the “up” or “down” direction of the arrows is not correlated to the inner color of these arrows, meaning that four possibilities should be

[‡] In the case of the example in b-e), between the two groups attached to the C₂ carbon atom of the TCBD (*i.e.*, the R and the dicyano vinyl groups), the R group is arbitrarily considered to have a lower priority following the CIP priority rules.

considered: i) a red arrow pointing up filled with orange color, ii) a blue arrow pointing down filled with orange color, iii) a red arrow pointing up filled with green color, and iv) a blue arrow pointing down filled with green color.



Using this representation,[§] 24 stereoisomers can be identified in the case of the SubPc *M* isomer of **1** and an equal number of enantiomers for the *P* isomer (Figure S3.3).

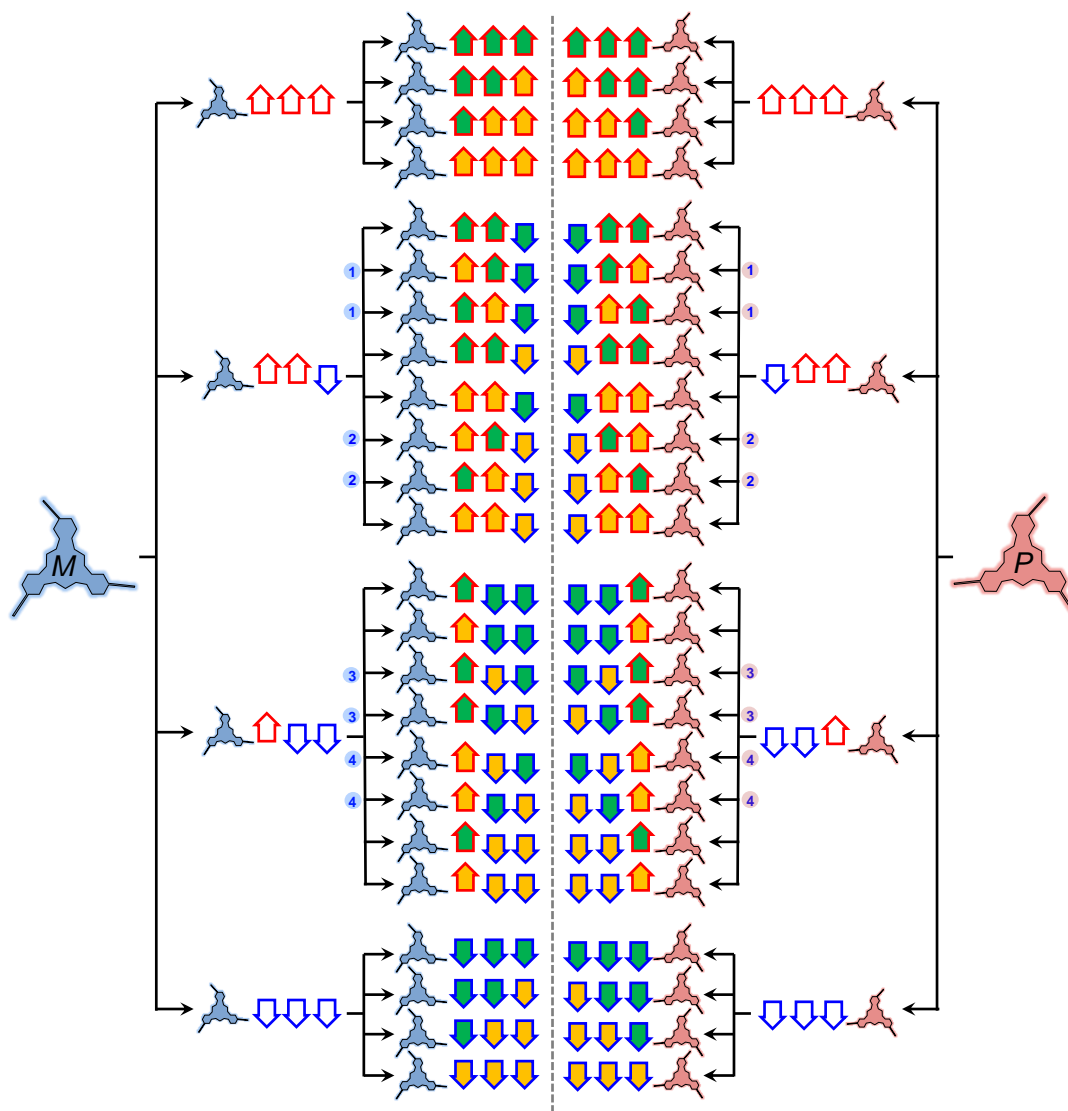


Figure S3.3. Cartoon representing the possible stereoisomers of *M* (left hand-side with respect to the vertical dashed line) and *P* (right hand-side with respect to the vertical dashed line) of (TCBD-aniline)₃-SubPc(^tBuPhO) **1**. Next to some stereoisomers, couples of numbers (from 1 to 4) have

[§] In the case of the conformers resulting from the rotation around the C-C single bond connecting the SubPc to the TCBD units, only the two more energetically-stable conformers, that is, one having the *N,N'*-dimethyl-aniline moiety pointing to the same side to which the SubPc axial ligand points to (*i.e.*, red arrow pointing up), and another one having the same moiety pointing at the opposite side to which the SubPc axial ligand points to (*i.e.*, blue arrow pointing down), have been taken into account.

been placed. Each couple of numbers indicates the two stereoisomers which have the same number of R_a and S_a , and aniline “up” and “down” elements, although differently arranged around the bowl-shape structure of the SubPc (*vide infra*).

It is important to notice here that some of the stereoisomers in Figure S3.3 (the ones indicated by a number from 1 to 4) could, at first sight, appear conformationally/configurationaly identical, and thus isoenergetic, since they present the same number of R_a and S_a , and aniline “up” and “down” elements.

However, the fact that each of the three TCBD units i) has a chiral axis that can be R_a or S_a , ii) is attached to a C_3 -symmetric SubPc, either M or P , and iii) is flanked by the other two TCBDs, makes the pair of stereoisomers not equivalent, and thus not isoenergetic.

For example, by looking at the two stereoisomers below (the two indicated in Figure S3.3 with the number 1, left-hand side), it is possible to clearly see that they are not equivalent.**



The four possible conformers of the S_a, S_a, S_a isomer of P -(TCBD-aniline)₃-SubPc(^tBuPhO) **1** resulting from the 180° rotation of each of the three TCBDs around the C-C single bond connecting the SubPc to the tetracyano unit are presented in Figure S3.4.

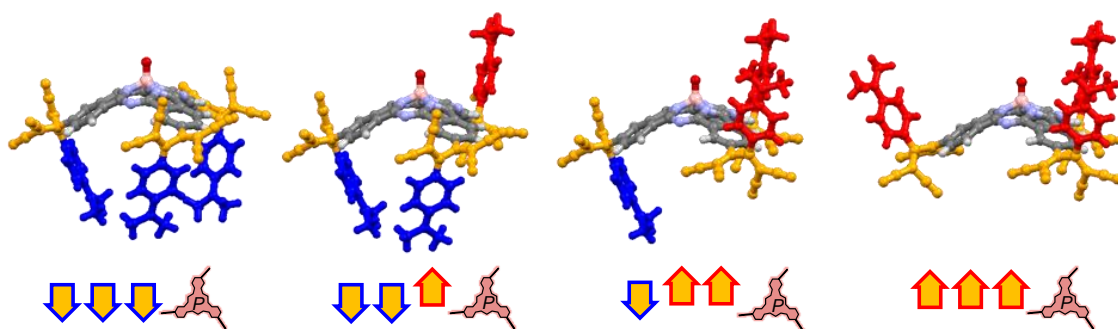


Figure S3.4. Molecular modeling structures (top) and cartoon representation (bottom) of the four possible conformers[§] of the S_a, S_a, S_a isomer of P -(TCBD-aniline)₃-SubPc(^tBuPhO) **1**. The conformers are obtained from the conformer on the left hand-side by 180° rotation of each of the three peripheral TCBD units around the C-C single bond connecting the SubPc to the TCBD.

** In this three-dimensional representation of the two stereoisomers offered, the chiral information of each of the three TCBD units is represented with an arrow either at the right- (green-filled arrow, R_a) or left-hand (orange-filled arrow, S_a) side of the line laterally departing from the SubPc). Moreover, arrows pointing towards (blue arrow) or away from (red arrow) the SubPc refers to the N, N' -dimethyl-aniline moiety pointing to the same side to which the SubPc axial ligand points to or at the opposite side to which the SubPc axial ligand points to, respectively.

Please note that rotation around this C-C bond does not modify the S_a configuration of the chiral axis of the three TCBD units.^{††}

In another example, the four possible stereoisomers of the S_a, S_a, S_a isomer of P -(TCBD-aniline)₃-SubPc(^tBuPhO) **1** resulting from the inversion (from S_a to R_a) of each of the three peripheral TCBD units are presented in Figure S3.5.

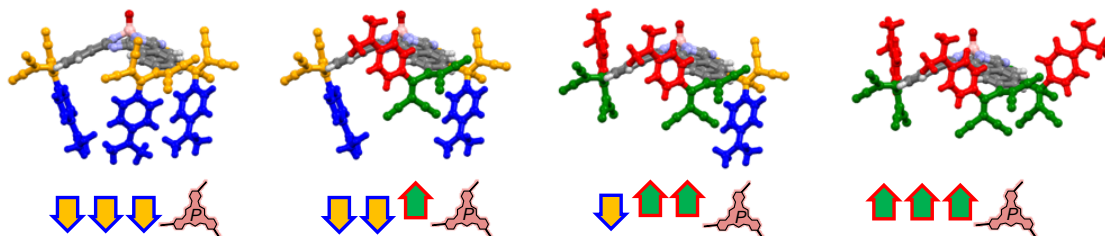


Figure S3.5. Molecular modeling structures (top) and cartoon representation (bottom) of the S_a, S_a, S_a isomer of P -(TCBD-aniline)₃-SubPc(^tBuPhO) **1** with the three N,N' -dimethyl-aniline moieties pointing at the opposite side to which the SubPc axial ligand points to (left hand-side structure), and the three possible stereoisomers resulting from the configuration inversion (from S_a to R_a) of each of the three peripheral TCBD units. Please note that each S_a to R_a TCBD inversion is accompanied by the change of the side to which the N,N' -dimethyl-aniline points to (*i.e.*, from opposite to the SubPc axial ligand, to the same side).^{††}

It is important to mention here that the 24 stereoisomers of P -(TCBD-aniline)₃-SubPc(^tBuPhO) **1** (Figure S3.3) could, in principle, interconvert between them by i) S_a/R_a configurational inversion, and/or ii) rotation around the around the C-C single bond connecting the SubPc to the TCBD. The same holds for the 24 stereoisomers of M -(TCBD-aniline)₃-SubPc(^tBuPhO) **1**.^{‡‡}

While considering the equilibrium between the different stereoisomers in **1** (and the same also applies to **2**), several interconversion pathways should be considered. For example, in Figure S3.6, the two possible pathways transforming one conformer of the S_a, S_a, S_a isomer of P -(TCBD-aniline)₃-SubPc(^tBuPhO) **1** into another conformer of the S_a, S_a, R_a isomer of P -(TCBD-aniline)₃-SubPc(^tBuPhO) **1** are presented.

^{††} For an easier visualization of the conformers, i) the SubPc axial ^tBuPhO ligand has been omitted, except for the oxygen atom (colored in red), ii) the TCBD units have been colored in either orange or green depending if they present a S_a (orange) or R_a (green) configuration, and iii) the N,N' -dimethyl-aniline moiety has been colored in either blue or red depending if this group is pointing to the same side to which the SubPc axial ligand points to (red) or to the opposite one (blue).

^{‡‡} It should be taken into account that no interconversion between the P and M stereoisomers of (TCBD-aniline)₃-SubPc(^tBuPhO) **1** or (TCBD-aniline)₃-SubPc(TCBD-aniline) **2** is possible since this would imply i) the loss of the axial ^tBuPhO ligand in the case of **1**, or TCBD-aniline ligand in the case of **2**, by breaking the B-O axial bond in the case of **1**, or B-C axial bond in the case of **2**, ii) a bowl-to-bowl inversion of the resulting SubPc macrocycle, and iii) the reattachment of the axial ligand to the “inverted” SubPc by formation of a new B-O axial bond in the case of **1**, or B-C axial bond in the case of **2**.

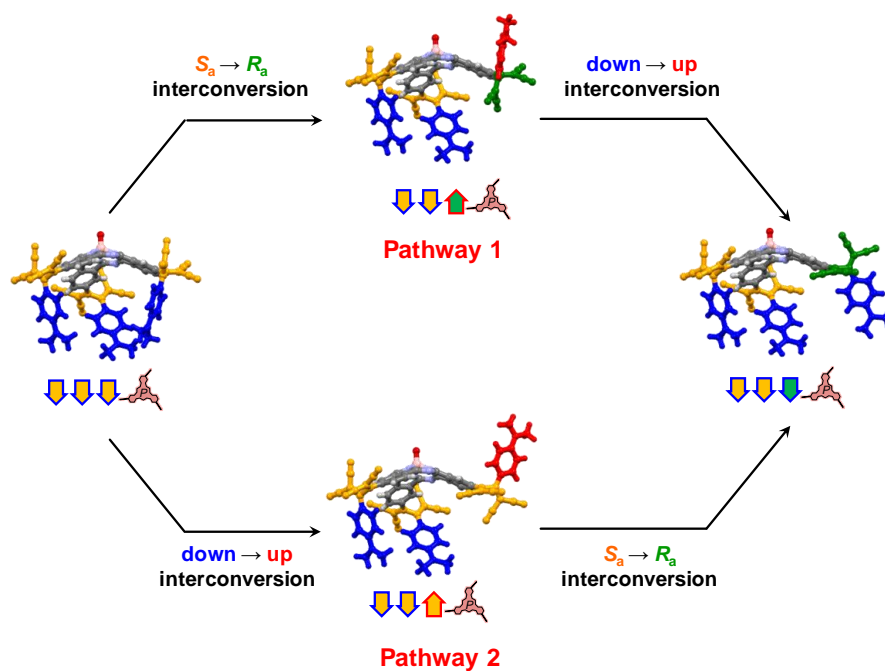


Figure S3.6. Molecular modeling structures and cartoon representation (below) of the S_a,S_a,S_a isomer of P -(TCBD-aniline)₃-SubPc(^tBuPhO) **1** with the three N,N' -dimethyl-aniline moieties pointing at the opposite side to which the SubPc axial ligand points to (left hand-side structure) and the two possible interconversion pathways both leading to the formation of a S_a,S_a,R_a isomer of P -(TCBD-aniline)₃-SubPc(^tBuPhO) **1** with the three N,N' -dimethyl-aniline moieties pointing at the opposite side to which the SubPc axial ligand points to (right hand-side structure). Pathway 1 involves i) the S_a to R_a configuration inversion of one TCBD unit followed by ii) 180° rotation of the same TCBD unit around the C-C single bond that connects it to the SubPc. Pathway 2 involves i) the 180° rotation of one TCBD unit around the C-C single bond that connects it to the SubPc followed by ii) a S_a to R_a configuration inversion of the same TCBD unit.^{††}

In the case of the racemic mixture of M and P isomers of (TCBD-aniline)₃-SubPc(TCDB-aniline) **2**, an additional TCDB-aniline unit is present (in this case, at the SubPc axial position) with respect to (TCBD-aniline)₃-SubPc(^tBuPhO) **1**. As a consequence of this additional group, which can present either a S_a or R_a configuration, two new stereoisomers are expected for each of the stereoisomers identified for **1** so to have 48 stereoisomers in the case of the SubPc M isomer of **2** and an equal number of enantiomers for the P isomer.^{§§}

^{§§} Considering the SubPc geometry, rotation around the axial C-C single bond connecting the SubPc boron atom to the TCBD is not expected to give rise to conformers with substantially different stabilities.

4. Electrochemical characterization of (TCBD-aniline)-based SubPcs **1** and **2**, and (ethynyl-aniline)-based SubPc **3**.

Table S4.1. Electrochemical oxidation and reduction (V vs Fc⁺/Fc) for SubPcs **1-3** and phenyl-TCBD-aniline reference **4** detected by SWV at room temperature in 0.2 M (for SubPc **1-3**) and 0.1 M (for **4**) solutions of *n*-Bu₄NPF₆ in dichloromethane.

| | E_{ox}^3 | E_{ox}^2 | E_{ox}^1 | E_{red}^1 | E_{red}^2 | E_{red}^3 | E_{red}^4 | E_{red}^5 |
|-----------------------|--------------------|--------------------|--------------------|--------------------|--------------------|--------------------|--------------------|--------------------|
| 1 | | +0.91 ^a | +0.85 ^b | -0.79 ^d | -1.11 ^d | -1.81 ^b | | |
| 2 | | +0.93 ^a | +0.88 ^b | -0.71 ^c | -0.81 ^d | -1.14 ^d | -1.31 ^c | -1.45 ^b |
| 3 | +0.71 ^b | +0.65 ^a | +0.41 ^b | -1.40 ^b | -1.85 ^b | -2.22 ^b | | |
| 4 ^g | | | +0.92 ^a | -0.94 ^d | -1.26 ^d | | | |

^aAniline-centered process. ^bSubPc-centered process. ^cTCBD_{axial}-centered process. ^dTCBD_{peripheral}-centered process.

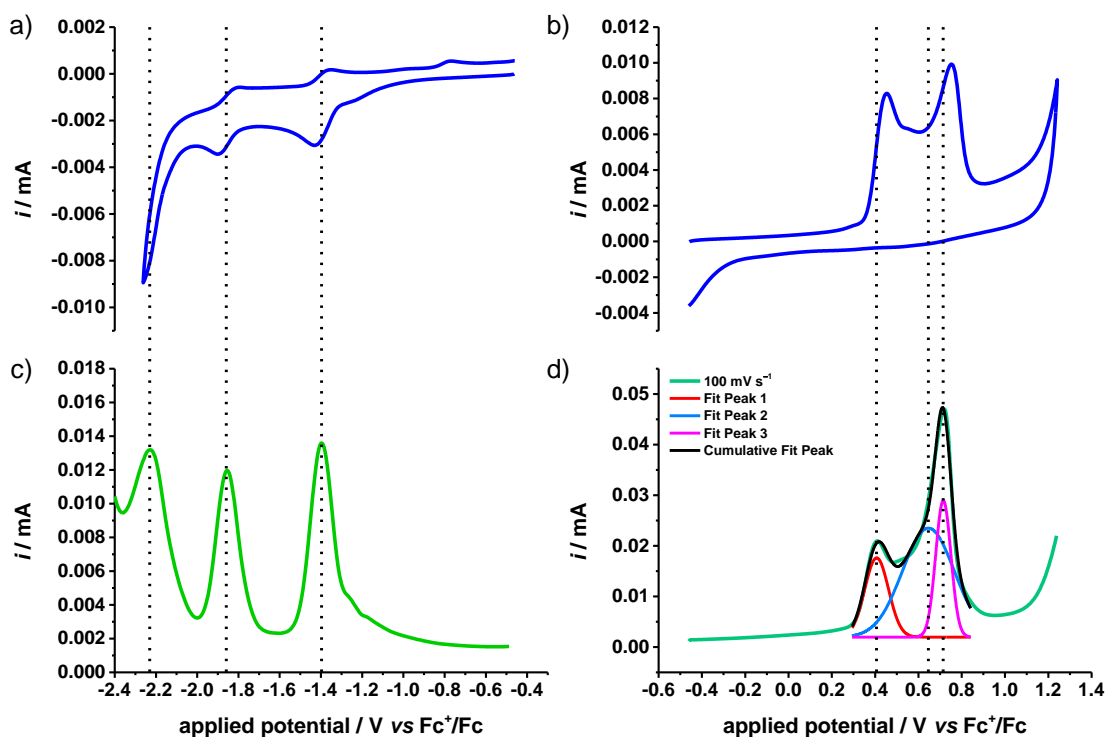


Figure S4.1. Cyclic (blue) and square wave voltammograms (green) of the reduction (left) and oxidation (right) of (ethynyl-aniline)₃-SubPc(BuPhO) **3** at scan rates of 50 mV s⁻¹ for a) and 100 mV s⁻¹ for b), c), and d) in a 0.2 M solution of *n*-Bu₄NPF₆ in dichloromethane. Chemical potentials are referred to $E_{1/2}$ of the Fc⁺/Fc redox couple. The oxidation peaks in d) were obtained by multiple GAUSS peak fittings.

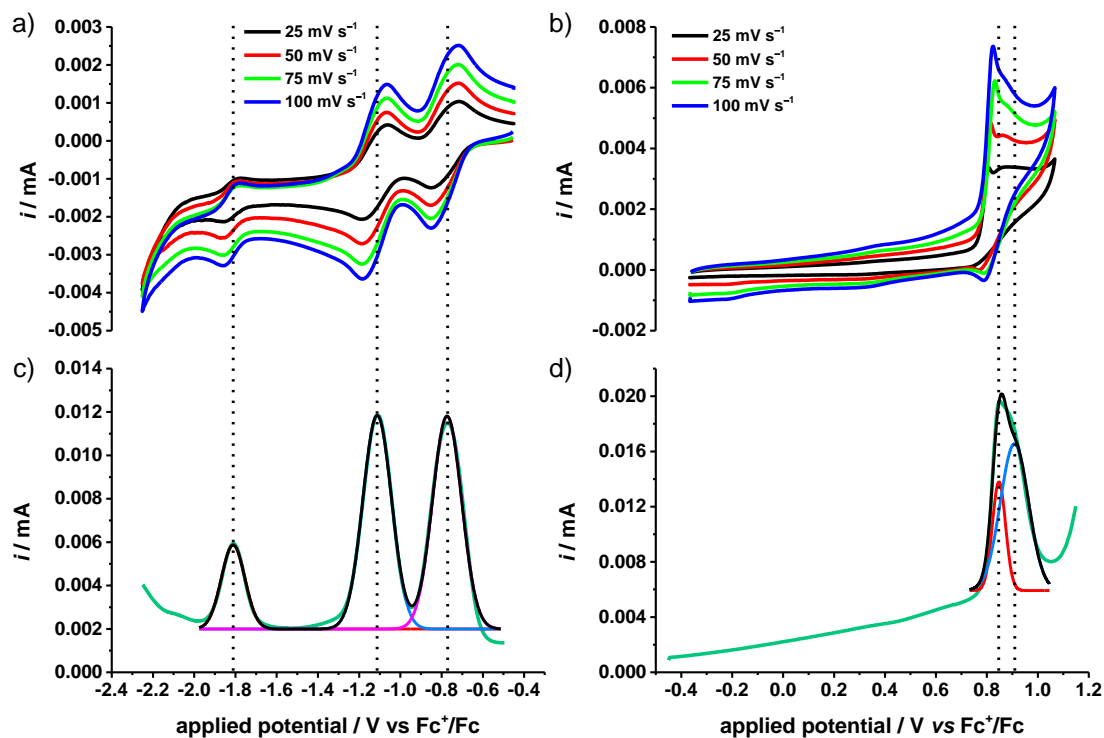


Figure S4.2. Cyclic (top) and square wave voltammograms (bottom) of the reduction (left) and oxidation (right) of (TCBD-aniline)₃-SubPc(*t*BuPhO) **1** at scan rates between 25 and 100 mV s⁻¹ for a) and b) and 100 mV s⁻¹ for c) and d) in a 0.2 M solution of *n*-Bu₄NPF₆ in dichloromethane. Potentials are referred to *E*_{1/2} of the Fc⁺/Fc redox couple. The reductions and oxidations in c) and d) were obtained by multiple GAUSS peak fittings.

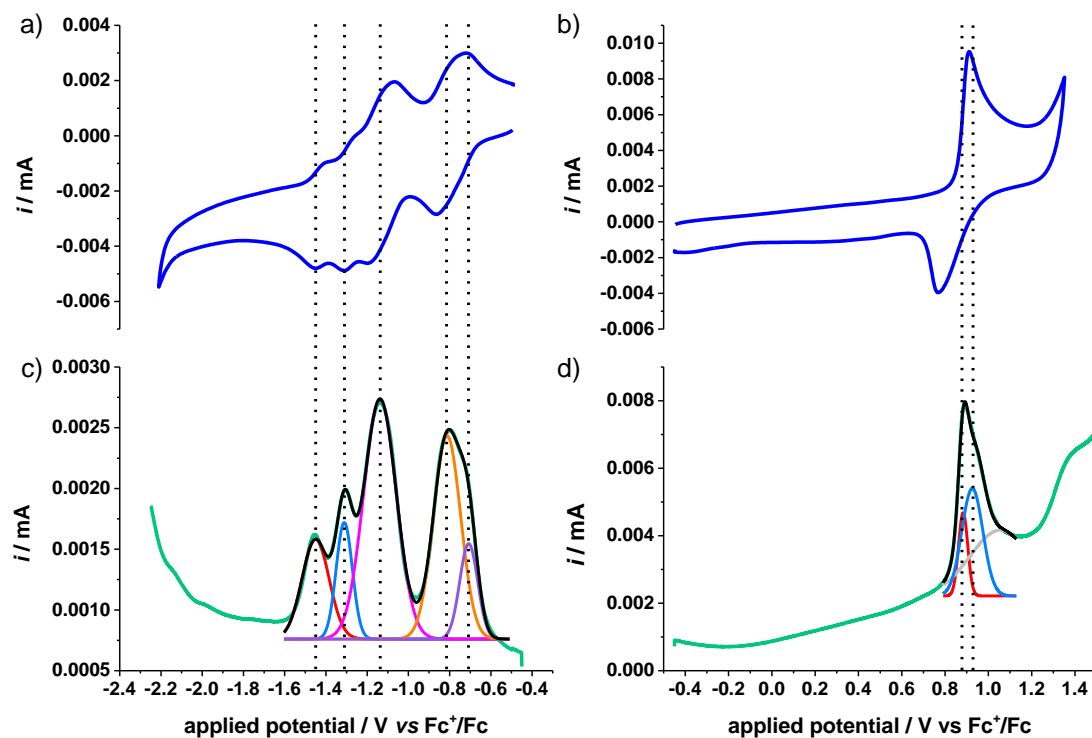


Figure S4.3. Cyclic (blue) and square wave voltammograms (green) of the reduction (left) and oxidation (right) of (TCBD-aniline)₃-SubPc(TCBD-aniline) **2** at scan rates of 100 mV s⁻¹ for a) and b), 25 mV s⁻¹ for c), and 12.5 mV s⁻¹ for d) in a 0.2 M solution of *n*-Bu₄NPF₆ in dichloromethane. Potentials are referred to $E_{1/2}$ of the Fc⁺/Fc redox couple. The reductions and oxidations in c) and d) were obtained by multiple GAUSS peak fittings.

5. Photophysical characterization of (TCBD-aniline)-based SubPcs 1 and 2, and reference compounds 3 and 4.

Table S5.1. Ground state absorption characteristics of (TCBD-aniline)₃-SubPc(^tBuPhO) **1**, (TCBD-aniline)₃-SubPc(TCBD-aniline) **2**, (ethynyl-aniline)₃-SubPc(^tBuPhO) **3**, and phenyl-TCBD-aniline **4**.

| com pou nd | solvent | Q-band | | n → π* transition (3) / CT band (1, 2, 4) | | Soret band | | NIR absorption | |
|----------------------|---------------|--------------------------|---|--|---|-----------------------|---|--------------------------|--|
| | | λ _{max} / nm | ε / M ⁻¹ cm ⁻¹ | λ _{max} / nm | ε / M ⁻¹ cm ⁻¹ | λ _{max} / nm | ε / M ⁻¹ cm ⁻¹ | λ _{max} / nm | ε / M ⁻¹ cm ⁻¹ |
| 1 | toluene | 622 | 64621 | 462 | 68733 | 310 (342) | 48747 | 860 | 619 |
| | chlorobenzene | 622 | 64706 | 468 | 77776 | 312 (344) | 50519 | 865 | 1710 |
| | anisole | 624 | 68251 | 470 | 78098 | 311 (342) | 54235 | 861 | 1674 |
| | benzonitrile | 620 | 63419 | 473 | 77950 | 315 (343) | 51589 | 845 | 1633 |
| 2 | chlorobenzene | 636 | 50165 | 472 | 105608 | 312 (343) | 58833 | 838 | 5328 |
| | anisole | 636 | 50929 | 475 | 106937 | 313 (341) | 61746 | 832 | 5496 |
| | benzonitrile | 638 | 39805 | 473 | 86307 | 313 (342) | 49308 | 860 | 4802 |
| 3 | toluene | 601 | 156655 | 439 | 35487 | 329 | 122606 | - | - |
| | chlorobenzene | 605 | 108345 | 448 | 26510 | 332 | 92540 | - | - |
| | anisole | 604 | 123611 | 447 | 28806 | 332 | 101872 | - | - |
| | benzonitrile | 607 | 107020 | 455 | 26441 | 334 | 90435 | - | - |
| 4⁹ | toluene | - | - | 462 | 24369 | - | - | - | - |
| | benzonitrile | - | - | 477 | 24325 | - | - | - | - |

Table S5.2. Fluorescence quantum yield (Φ_F) and fluorescence maxima of (TCBD-aniline)₃-SubPc(^tBuPhO) **1**, (TCBD-aniline)₃-SubPc(TCBD-aniline) **2**, and (ethynyl-aniline)₃-SubPc(^tBuPhO) **3** in different solvents.

| solvent | solvent polarity E _T ^N | 1 | | 2 | | 3 | |
|---------------|---|-----------------------|--------------------------|-----------------------|--------------------------|--------------------|-----------------------|
| | | Φ _F / % | λ _{max} / nm | Φ _F / % | λ _{max} / nm | Φ _F / % | λ _{max} / nm |
| toluene | 0.099 | 0.02 | 650 | - | - | 27 | 613 |
| chlorobenzene | 0.188 | 0.02 | 655 | < 10 ⁻³ | ~666 | 11 | 624 |
| anisole | 0.198 | 0.05 | 658 | < 10 ⁻³ | ~668 | 9.6 | 623 |
| benzonitrile | 0.333 | 0.01 | 663 | < 10 ⁻³ | ~664 | 0.12 | 623 |

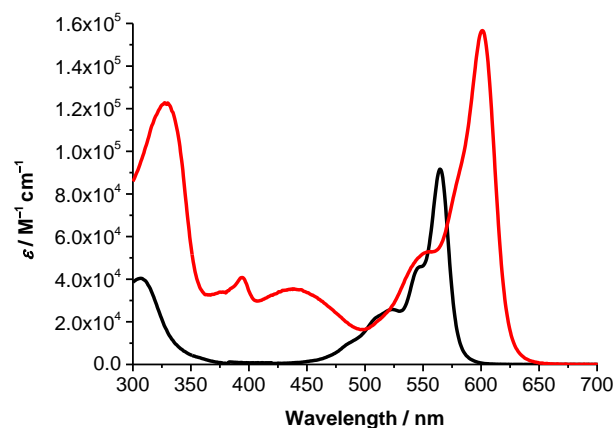


Figure S5.1. Steady-state absorption spectra of (ethynyl-aniline)₃-SubPc(^tBuPhO) **3** (red) and H₁₂SubPc(Cl) (black) in toluene.

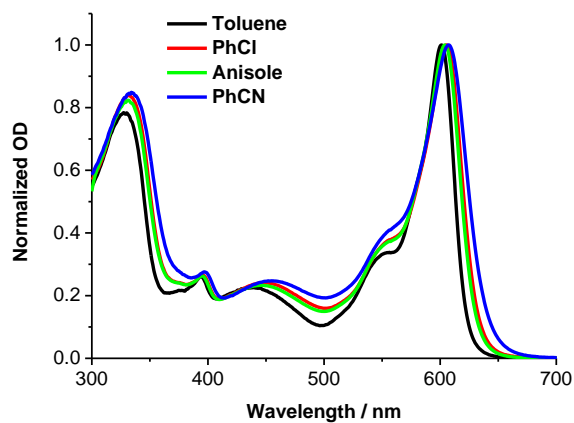


Figure S5.2. Normalized (with respect to SubPc *Q*-band) steady-state absorption spectra of (ethynyl-aniline)₃-SubPc(^tBuPhO) **3** in toluene (black), chlorobenzene (red), anisole (green), and benzonitrile (blue).

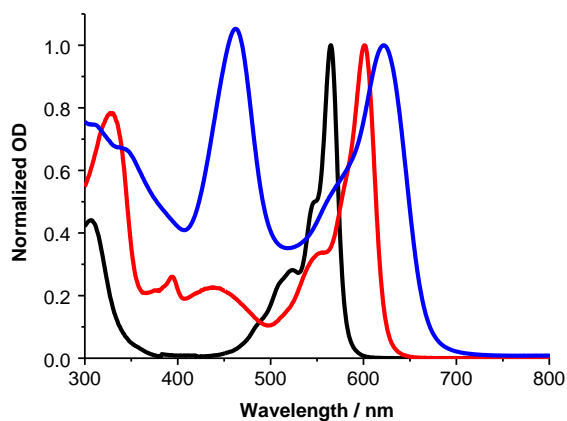


Figure S5.3. Normalized (with respect to SubPc *Q*-band) steady-state absorption spectra of (TCBD-aniline)₃-SubPc('BuPhO) **1** (blue), (ethynyl-aniline)₃-SubPc('BuPhO) **3** (red), and H₁₂SubPc(Cl) (black) in toluene.

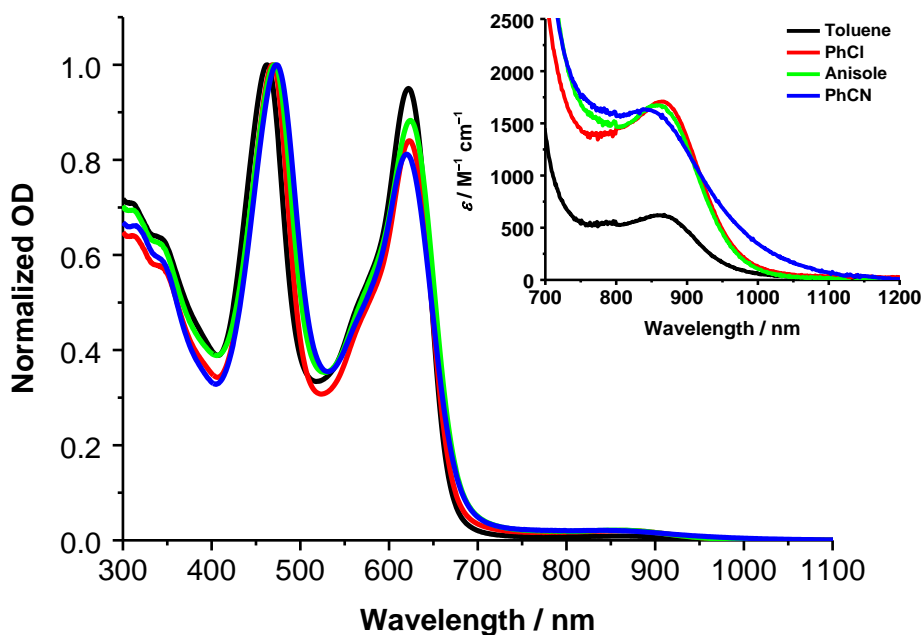


Figure S5.4. Normalized (with respect to TCBD-aniline CT band) steady-state absorption spectra of (TCBD-aniline)₃-SubPc('BuPhO) **1** in toluene (black), chlorobenzene (red), anisole (green), and benzonitrile (blue). Inset: Zoom of the steady-state absorption spectra in the region between 700 and 1200 nm.

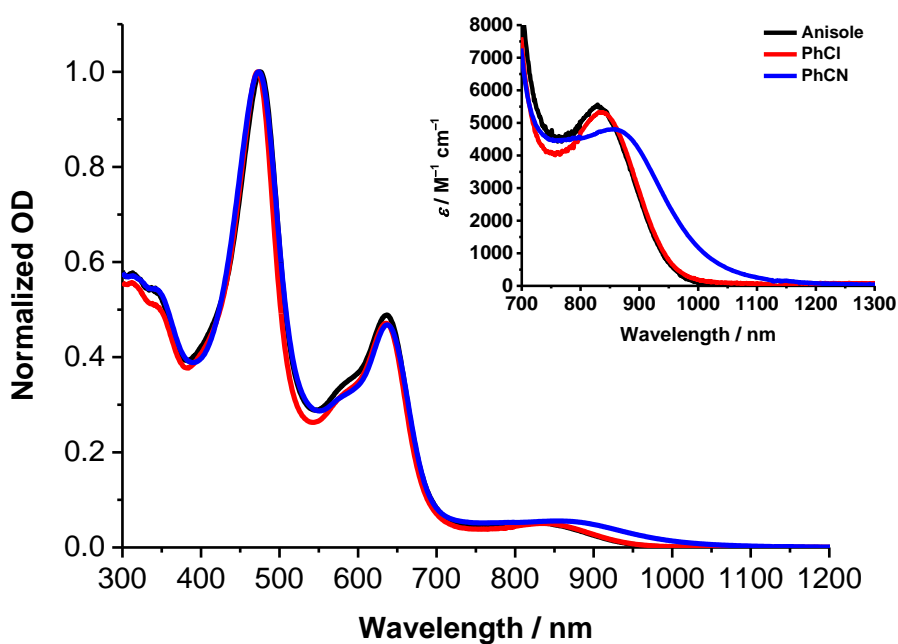


Figure S5.5. Left: Normalized (with respect to TCBD-aniline CT band) steady-state absorption spectra of (TCBD-aniline)₃-SubPc(TCBD-aniline) **2** in anisole (black), chlorobenzene (red), and benzonitrile (blue). Inset: Zoom of the steady-state absorption spectra in the region between 700 and 1200 nm.

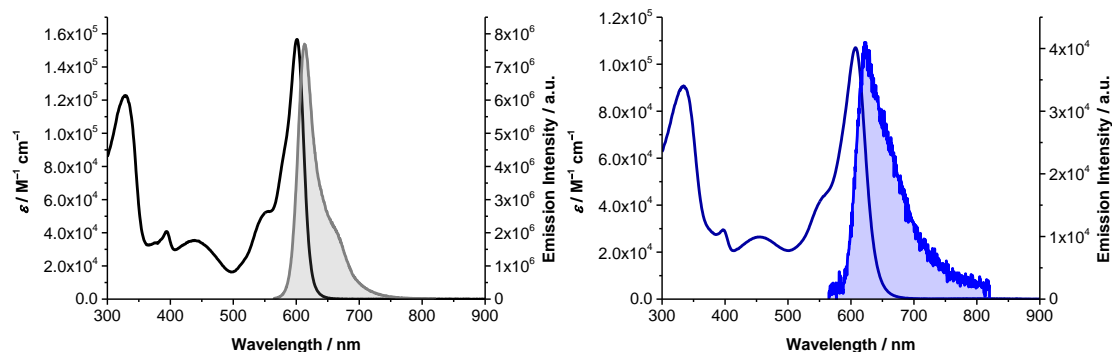


Figure S5.6. Steady-state absorption and fluorescence spectra of (ethynyl-aniline)₃-SubPc(BuPhO) **3** ($\lambda_{\text{ex}} = 550$ nm) in toluene (left, $c = 7.07 \times 10^{-7}$ M) and benzonitrile (right, $c = 9.38 \times 10^{-7}$ M).

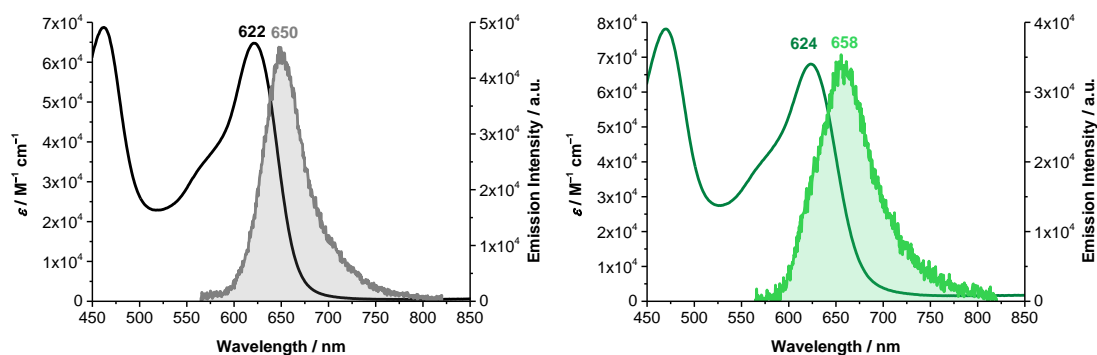


Figure S5.7. Steady-state absorption and fluorescence spectra of (TCBD-aniline)₃-SubPc(BuPhO) **1** ($\lambda_{\text{ex}} = 550$ nm, $c = 1.24 \times 10^{-6}$ M) in toluene (left) and anisole (right).

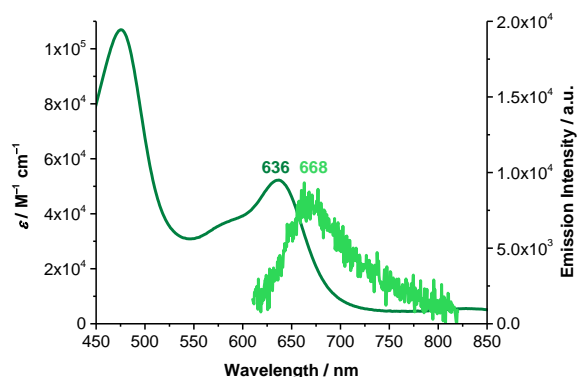


Figure S5.8. Steady-state absorption and fluorescence spectra of (TCBD-aniline)₃-SubPc(TCBD-aniline) **2** ($\lambda_{\text{ex}} = 470$ nm, $c = 9.38 \times 10^{-7}$ M) in anisole.

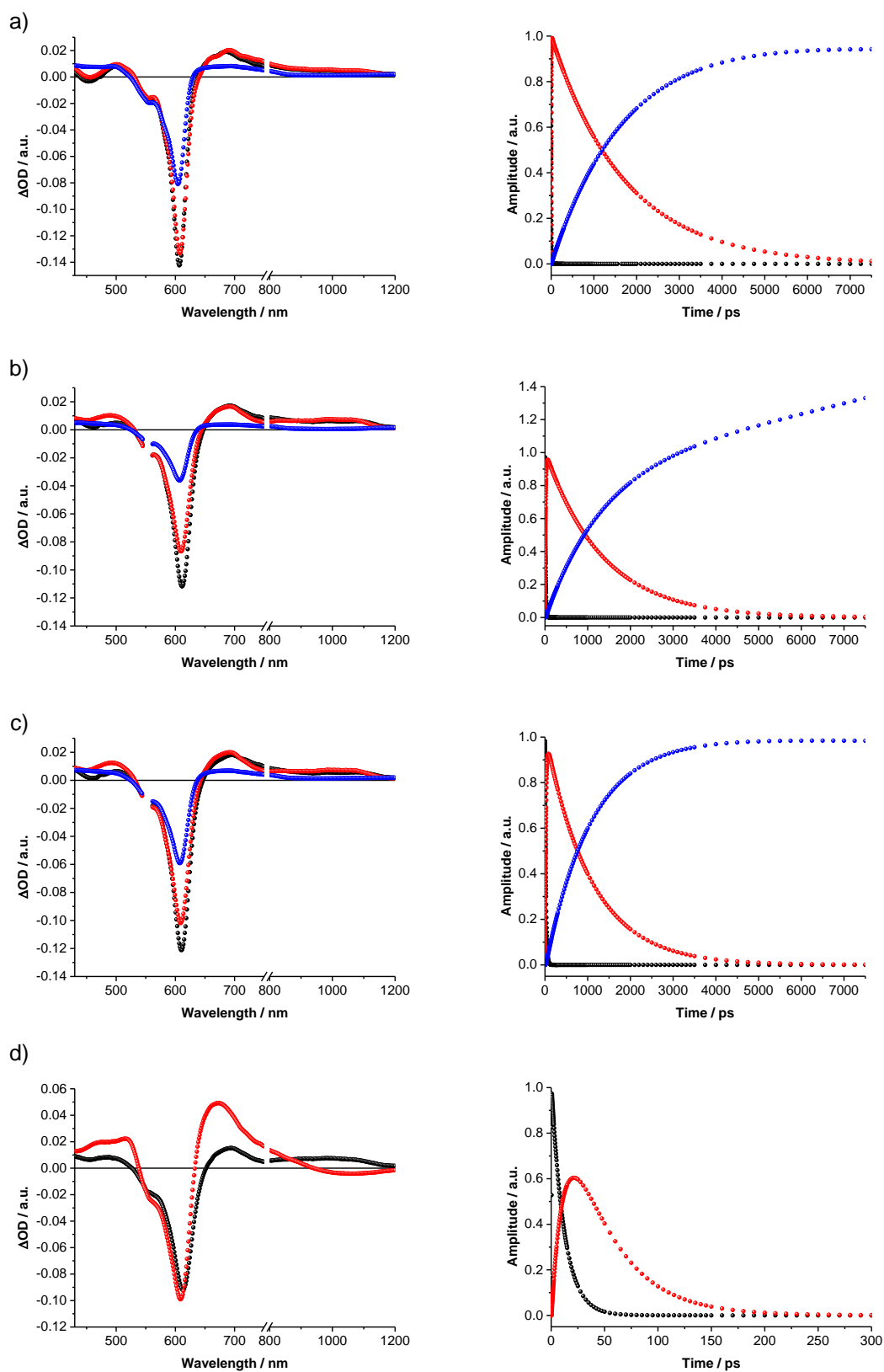


Figure S5.9. Evolution associated spectra (left) and associated time-dependent amplitudes (right) obtained upon femtosecond flash photolysis (550 nm, 400 nJ) of (ethynyl-aniline)₃-SubPc(BuPhO) **3** (2×10^{-5} M) in argon-saturated a) toluene, b) chlorobenzene, and c) anisole

monitoring intersystem crossing as well as d) benzonitrile monitoring charge separation and charge recombination.

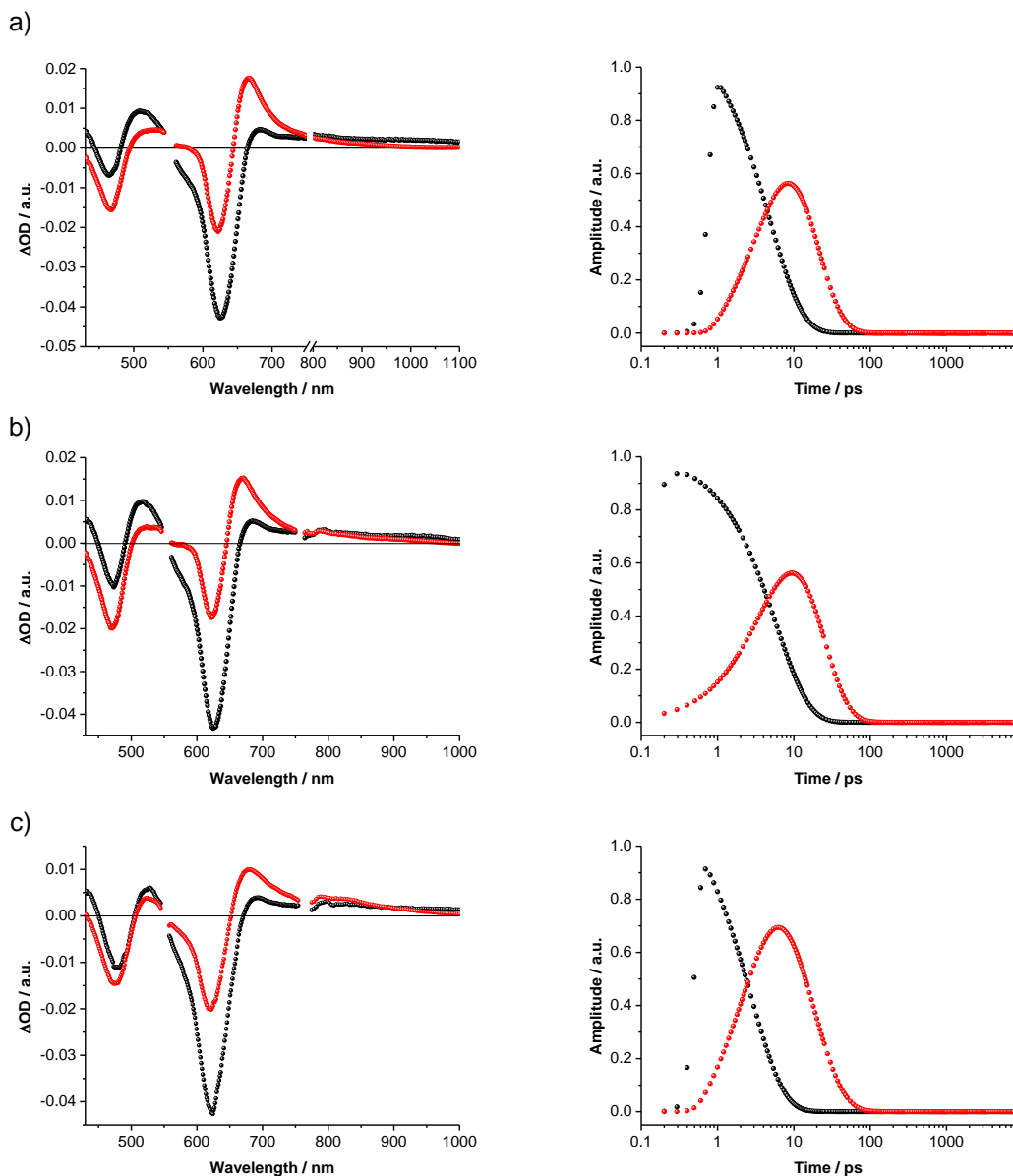


Figure S5.10. Evolution associated spectra (left) and associated time-dependent amplitudes (right) obtained upon femtosecond flash photolysis (550 nm, 400 nJ) of (TCBD-aniline)₃-SubPc('BuPhO) **1** (2×10^{-5} M) in argon-saturated a) toluene, b) chlorobenzene, and c) benzonitrile monitoring formation and decay kinetics.

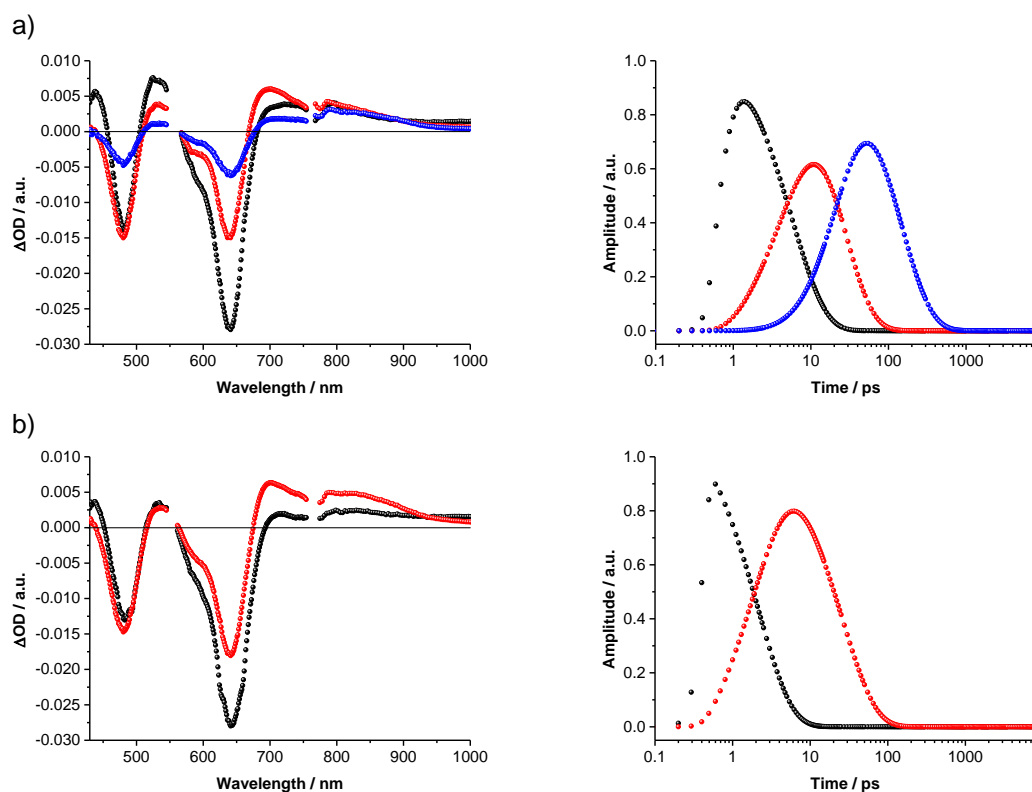


Figure S5.11. Evolution associated spectra (left) and associated time-dependent amplitudes (right) obtained upon femtosecond flash photolysis (550 nm, 400 nJ) of (TCBD-aniline)₃-SubPc((TCBD-aniline) **2** (3×10^{-5} M) in argon-saturated a) chlorobenzene and b) benzonitrile (bottom) monitoring formation and decay kinetics.

6. Supporting Information References.

- 1 L. Feng, M. Rudolf, O. Trukhina, Z. Slanina, F. Uhlik, X. Lu, T. Torres, D. M. Guldi and T. Akasaka, *Chem. Commun.*, 2015, **51**, 330.
- 2 J. J. Snellenburg, S. Laptinok, R. Seger, K. M. Mullen and I. H. M. van Stokkum, *J. Stat. Soft.*, 2012, **49**, 1.
- 3 K. M. Mullen and I. H. M. van Stokkum, *J. Stat. Soft.*, 2007, **18**, 1.
- 4 I. H. M. van Stokkum, D. S. Larsen and R. van Grondelle, *Biochim. Biophys. Acta* 2004, **1657**, 82.
- 5 D. Gonzalez-Rodriguez, T. Torres, D. M. Guldi, J. Rivera, M. A. Herranz and L. Echegoyen, *J. Am. Chem. Soc.*, 2004, **126**, 6301.
- 6 C. G. Claessens, M. J. Vicente-Arana and T. Torres, *Chem. Commun.*, 2008, 6378.
- 7 C. G. Claessens, D. Gonzalez-Rodriguez, B. del Rey, T. Torres, G. Mark, H. P. Schuchmann, C. von Sonntag, J. G. MacDonald and R. S. Nohr, *Eur. J. Org. Chem.*, 2003, 2547.
- 8 A. R. Lacy, A. Vogt, C. Boudon, J.-P. Gisselbrecht, W. B. Schweizer and F. Diederich, *Eur. J. Org. Chem.*, 2013, **2013**, 869.
- 9 M. Sekita, B. Ballesteros, F. Diederich, D. M. Guldi, G. Bottari and T. Torres, *Angew. Chem. Int. Ed.*, 2016, **55**, 5560.